```
AD-A110 035   LOCKHEED-GEORGIA CO  MARIETTA                                   F/G 20/4
              NUMERICAL AIRCRAFT DESIGN USING 3-D TRANSONIC ANALYSIS WITH OPT--ETC(U)
              AUG 81  A J SROKOWSKI, M E LORES, P AIDALA        F33615-78-C-3014
UNCLASSIFIED  LG81ER0107-VOL-1                AFWAL-TR-81-3091-VOL-1        NL
```

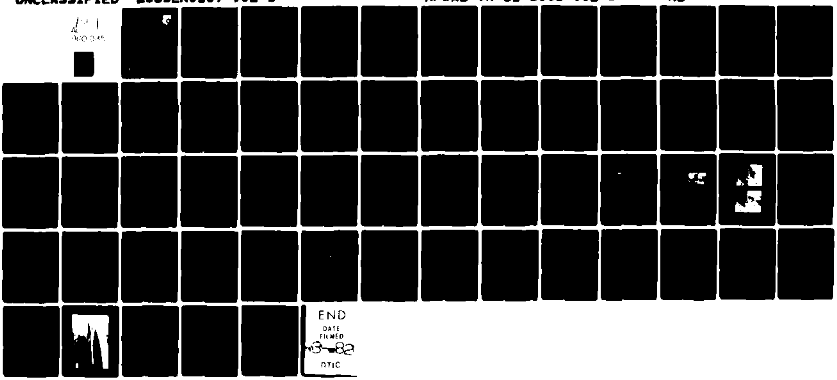

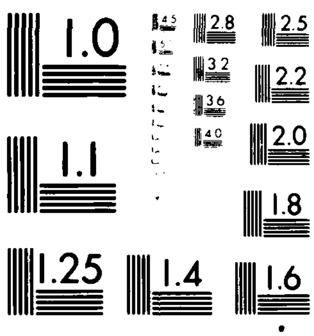

MICROCOPY RESOLUTION TEST CHART

[illegible]

AFWAL-TR-81-3091
VOLUME I

NUMERICAL AIRCRAFT DESIGN USING 3-D TRANSONIC ANALYSIS VITH OPTIMIZATION

)LUME I EXECUTIVE SUMMARY

LOCKHEED-GEORGIA COMPANY
86 SOUTH COBB DRIVE
MARIETTA, GEORGIA 30063

GRUMMAN AEROSPACE CORPORATION
BETHPAGE, NEW YORK 11714

AUGUST 1981
Final Report May 1978 to September 1980

FLIGHT DYNAMICS LABORATORY
AIR FORCE WRIGHT AERONAUTICAL LABORATORIES
AIR FORCE SYSTEMS COMMAND
WRIGHT PATTERSON AIR FORCE BASE, OHIO 45433

NOTICE

When Government drawings, specifications, or other data are used for any purpose other than in connection with a definitely related Government procurement operation, the United States Government thereby incurs no responsibility nor any obligation whatsoever; and the fact that the government may have formulated, furnished, or in any way supplied the said drawings, specifications, or other data, is not to be regarded by implication or otherwise as in any manner licensing the holder or any other person or corporation, or conveying any rights or permission to manufacture use, or sell any patented invention that may in any way be related thereto.

This report has been reviewed by the Office of Public Affairs (ASD/PA) and is releasable to the National Technical Information Service (NTIS). At NTIS, it will be available to the general public, including foreign nations.

This technical report has been reviewed and is approved for publication.

Robert A. Large

ROBERT A. LARGE, Capt, USAF
Project Engineer

Lowell C. Keel

LOWELL C. KEEL, Maj, USAF
Chief, Aerodynamics & Airframe Branch
Aeromechanics Division

FOR THE COMMANDER

John R. Chevalier

JOHN R. CHEVALIER, Colonel, USAF
Chief, Aeromechanics Division

"If your address has changed, if you wish to be removed from our mailing list, or if the addressee is no longer employed by your organization please notify AFWAL/FIMM, W-PAFB, OH 45433 to help us maintain a current mailing list".

Copies of this report should not be returned unless return is required by security considerations, contractual obligations, or notice on a specific document.

Unclassified

SECURITY CLASSIFICATION OF THIS PAGE (When Data Entered)

REPORT DOCUMENTATION PAGE

READ INSTRUCTIONS BEFORE COMPLETING FORM

1. REPORT NUMBER
AFWAL-TR-81-3091, VOLUME I

2. GOVT ACCESSION NO.
AD-A110 035

3. RECIPIENT'S CATALOG NUMBER

4. TITLE (and Subtitle)
NUMERICAL AIRCRAFT DESIGN USING 3-D TRANSONIC ANALYSIS WITH OPTIMIZATION
VOLUME I, EXECUTIVE SUMMARY

5. TYPE OF REPORT & PERIOD COVERED
Final Report
May 1978 - September 1980

6. PERFORMING ORG. REPORT NUMBER
LG81ER0107

7. AUTHOR(s)
A. J. Srokowski, M. E. Lores,
P. Aidala*

8. CONTRACT OR GRANT NUMBER(s)
F33615-78-C-3014

9. PERFORMING ORGANIZATION NAME AND ADDRESS
Lockheed-Georgia Company
86 South Cobb Drive
Marietta, Georgia 30063

10. PROGRAM ELEMENT, PROJECT, TASK AREA & WORK UNIT NUMBERS
62201F
24041026

11. CONTROLLING OFFICE NAME AND ADDRESS
Flight Dynamics Laboratory (AFWAL/FIMM)
Air Force Wright Aeronautical Laboratories
Wright-Patterson Air Force Base, Ohio 45433

12. REPORT DATE
August 1981

13. NUMBER OF PAGES
57

14. MONITORING AGENCY NAME & ADDRESS(if different from Controlling Office)

15. SECURITY CLASS. (of this report)
Unclassified

15a. DECLASSIFICATION DOWNGRADING SCHEDULE

16. DISTRIBUTION STATEMENT (of this Report)

Approved for public release; distribution unlimited.

17. DISTRIBUTION STATEMENT (of the abstract entered in Block 20, if different from Report)

18. SUPPLEMENTARY NOTES

*Grumman Aerospace Corporation
Bethpage, New York 11714

19. KEY WORDS (Continue on reverse side if necessary and identify by block number)

Aircraft	Wing Design	Numerical Optimization
Aerodynamics	Computational Aerodynamics	
Transonic Flow	Transonic Aircraft Design	
Optimization	Transonic Flow Analysis	

20. ABSTRACT (Continue on reverse side if necessary and identify by block number)

This executive summary volume highlights results obtained by the Lockheed-Georgia Co. and Grumman Aerospace Corp. under AFWAL Contract #F33615-78-C-3014. The purpose of the contract was to develop and validate a new transonic wing design procedure using the numerical optimization technique. The new procedure was used to design both a transport and a fighter configuration. Because the missions and design requirements of a fighter and transport are so different, the design procedure was developed along parallel lines. Lockheed-Georgia Co.

DD FORM 1 JAN 73 1473 EDITION OF 1 NOV 65 IS OBSOLETE

Unclassified

SECURITY CLASSIFICATION OF THIS PAGE (When Data Entered) developed the transport design procedure, and Grumman Aerospace Corp. developed the fighter design procedure.

This executive summary volume is divided into two parts: Part 1 highlights the transport development, and Part 2 highlights the fighter development. There are two other volumes which make up the final report. Volume 2 is the main volume in the final report. It presents in detail the information that has been highlighted here. Volume 2 is also divided into two parts with part 1 dealing with transport design and part 2 concerned with the fighter design. Volume 3 is a detailed user's guide to the computer programs produced under this contract. Volume 3 is similarly divided into two parts.

A detailed summary of the work performed in the Advanced Transonic Technology (ATT) program to incorporate 3-D Transonic computational aerodynamics methods into aircraft design procedures is presented. Existing transonic analysis programs were modified for the design procedure and linked with a numerical optimization program to design wings that are in some sense optimized for a given set of design conditions.

The design procedure was validated by applying it in two design case studies. The case studies selected were a transport design based on a derivative of the C141 B aircraft and a fighter design study based on the CDAF (Configuration Design of Advanced Fighters) program dual role configuration. The application of the design procedure in each of these case studies is described in detail. The configurations resulting from these studies were subjected to design verification wind tunnel testing. Comparisons of test data with computed results are presented.

PREFACE

This executive summary volume highlights results obtained by the Lockheed-Georgia Co. and Grumman Aerospace Corp. under AFWAL Contract #F33615-78-C-3014. The purpose of the contract was to develop and validate a new transonic wing design procedure using the numerical optimization technique. The new procedure was used to design both a transport and a fighter configuration. Because the missions and design requirements of a fighter and transport are so different, the design procedure was developed along parallel lines. Lockheed-Georgia Co. developed the transport design procedure, and Grumman Aerospace Corp. developed the fighter design procedure.

This executive summary volume is divided into two parts: Part 1 highlights the transport development, and Part 2 highlights the fighter development. There are two other volumes which make up the final report. Volume 2 is the main volume in the final report. It presents in detail the information that has been highlighted here. Volume 2 is also divided into two parts with part 1 dealing with transport design and part 2 concerned with the fighter design. Volume 3 is a detailed user's guide to the computer programs produced under this contract. Volume 3 is similarly divided into two parts.

Personnel who contributed to this contract effort are: Lockheed-Georgia Company, A. J. Srokowski, M. E. Lores, R. A. Weed and P. R. Smith; Grumman Aerospace Corp., P. Aidala.

The authors wish to acknowledge the assistance given by Capt. R. A. Large who was the AFWAL contract monitor.

TABLE OF CONTENTS

TABLE OF CONTENTS (CONT'D)

TABLE OF CONTENTS (CONT'D)

LIST OF ILLUSTRATIONS

LIST OF ILLUSTRATIONS (CONT'D)

SECTION I

INTRODUCTION

Computational aerodynamic methods that are significantly better than existing techniques are needed to design advanced aircraft configurations in a timely and cost-effective manner. The need for better methods is due in part to the demand for computational accuracy brought about by the increased aerodynamic sensitivity at transonic speeds of advanced technology concepts such as supercritical wings, active controls, variable camber wings, and laminar flow control. Also, improved aerodynamic tools are required to handle new configurational concepts such as (1) high aspect ratio wings, spanloader designs with thick wings, and winglets for transport-category aircraft; and, (2) swept forward wings, variable camber wings with direct lift control, canards, and blended-wing concepts for fighters. Because efficient transonic performance continues to be an important design requirement for military and commercial aircraft, there is also a particular need for improved transonic aerodynamic computational tools to accurately calculate the performance for each of these new technology and configurational concepts. The methods are also required because the increasing costs of wind tunnel tests together with the interference and scale problems associated with tests conducted at transonic conditions[1,2] make total reliance on experimental configuration development impractical.

Significant strides have been made in the development of 3-D transonic aerodynamic design and analysis codes over the past few years. Although many of the methods are still in the evolutionary stage, a few have matured to the point where application to the solution of aircraft design problems is practical [3,4,5].

The primary objective of the Advanced Transonic Technology (ATT) program was to demonstrate that performance improvements and/or reduced development time and costs can be achieved by incorporating 3-D transonic methods into aircraft design procedures. The attainment of the objective would result not only in very efficient advanced technology configurations which meet future Air Force mission requirements, but also would produce an experimentally verified, efficient, and documented transonic configuration design method.

The overall program approach and the individual tasks are summarized in Figure 1. As shown in that figure, the program was conducted by performing six technical tasks which were grouped into three time phases.

During Phase I, a fighter and a transport configuration employing advanced technology were selected. Also, during Phase I, the 3-D transonic analysis codes were evaluated, and necessary modifications for design procedure use were made.

Following Air Force approval of the selected configurations, computer codes, and the design procedure, the detailed configuration aerodynamic designs and wind tunnel tests were performed in Phase II. During the third and final phase: (1) wind tunnel data were used to determine mission performance; (2) theoretical predictions and experimental results were compared; and (3) a final production design procedure was developed.

SECTION II

TRANSPORT DESIGN

1. MISSION AND CONFIGURATION

At the start of the design study, the political and economic environment relative to military transport aircraft made the development of a derivative aircraft a more realistic prospect than the development of a completely new transport aircraft for which design requirements were not clearly defined. The derivative must, of course, exhibit significantly improved performance for the original mission, or increased ability to perform alternate missions.

a. Mission Definition and Design Goal

Operation of the USAF C-141 fleet accounts for approximately 15% of the total Air Force fuel allotment, so that aircraft modifications to improve its efficiency are of interest. Furthermore, because the general arrangement and mission of the C-141 are representative of current and planned military transports, aerodynamic technologies developed using the C-141 as a case study can be expected to be of general applicability.

A twin-engined active control derivative of the C-141B was selected as the case study aircraft. The derivative is designated herein as the C-141B/AC2; it is designed to carry a 75,000 pound payload 3,500 nautical miles at 0.80 Mach number. The cruise Mach number of 0.80 was selected instead of the 0.77 cruise Mach number of the C-141B to improve productivity and to provide a more challenging transonic design problem. Performance constraints include a field length of 7,500 feet and an initial cruise altitude of 35,000 feet. The targeted range and payload of the derivative aircraft are compared to those of the C-141B in Figure 2.

The design goal of this study was to significantly reduce the C-141B/AC2 empty weight (OWE) and fuel requirements from those of the C-141B.

b. Configuration Development

The C-141B/AC2 configuration was sized using the Lockheed-Georgia General Aircraft Sizing Program (GASP), a proprietary computer program presently used for all company preliminary design studies. The program accounts for the interaction of the various design constraints and technical disciplines involved in the aircraft design process. Technology levels for the various disciplines are controlled by the use of input adjusting factors. The C-141B/AC2 aircraft has been sized using advanced technology levels which are appropriate to an initial operational capability date in the mid-1980s.

A matrix of configuration variables was examined to determine the minimum fuel aircraft which met the design mission. The range of variables considered was:

Wing Loading	100 to 140 LB/FT^2
Aspect Ratio	8 to 12
Wing Sweep	10 to 25 DEG
Initial Cruise Altitude	31,000 to 35,000 FT
Cruise Power Setting	0.7 to 1.0

The constraints imposed on the parametric designs were:

Fuel Volume Ratio	$\geq$	1.0
(Fuel Volume Available/Fuel Required for 3500 NM)		
Field Length	$\leq$	7,500 FT
Aspect Ratio	$\leq$	12
Cruise Altitude	$\geq$	31,000 FT

c. Configuration Characteristics and Performance

The general arrangement of the C-141B/AC2 is shown in Figure 3. Technology level estimates were used in the GASP computer program to predict the C141B/AC2 configuration and performance. Based on these estimates, the C-141B/AC2 targeted OWE is approximately 80% of the C-141B and the targeted C-141B/AC2 fuel use is 64% of the fuel used by the C-141B. Predicted wing configuration is aspect ratio of 12, quarter chord sweep of 25° and an average thickness to chord ratio of .109. We will show later that by using the new design procedure, we obtained a wing significantly thicker than .109, but with only minor performance degradations.

d. Impact of Advanced Technologies

The C-141B/AC2 performance discussed above is made possible by the incorporation of the following advanced technologies:

- o High Aspect Ratio, Supercritical Wing
- o Advanced Engines
- o Composite Materials
- o Active Controls

The performance improvement as reflected in reduced fuel and gross weight brought about by each of the technologies is shown in Figure 4. Clearly, the major performance improvements result from the use of modern engines and advanced technology high aspect ratio wing. The C-141B/AC2 wing cruise aerodynamic design forms the basis for the validation of the transport design procedure.

2. DESIGN PROCEDURES

The transport wing design procedure is shown schematically in Figure 5. The procedure is based upon the use of an isolated wing code for the transonic design, and the use of a more economical subsonic panel method which provides good geometric resolution to compute interference pressures. (Example: On lower wing surface due to gear pod.)

The key element in the procedure is the use of numerical optimization in the wing design. The wing design code was developed by linking Vanderplaats' constrained function minimization program[6] with three-dimensional isolated wing analysis codes. Both an extended small disturbance code based on a program written by Bailey, Ballhaus, and Frick[7] and Jameson's FLO22 full potential equation program[8] were used in this study. The design objectives and constraints, and the permissible geometric perturbations (i.e., design variables) are detailed in the following paragraphs.

a. Design Objective and Constraints

To avoid the use of inaccurately calculated quantities such as drag in the optimization procedure, the design method was developed to permit the design of wings with specified chordwise pressure distributions. The design objective which worked best was the minimization of the RMS deviation between the target and actual pressures:

$$OBJ_1 = \left[\sum_N (C_P - C_{P_D})^2 / N \right]^{1/2}$$

where N is the number of pressure coefficients, and C_{P_D} is the target pressure coefficient.

b. Design Variables

Consistent with established wing geometry definition procedures, the wing geometry is determined by specifying the airfoil sections at various geometric control span stations and connecting these sections by linear loft elements. At each control station, 14 surface perturbation functions were used. The magnitude of each of these 14 surface perturbation functions plus the section twist angle are the fifteen design variables available for each surface at each geometric control span station. Thus, for a four control station wing, if all the surface perturbations were used, and if all the sections were designed simultaneously, a total of 15 variables per surface per station x 2 surfaces x 4 stations = 120 design variables, would be required.

c. Implementation

The simultaneous use of 120 design variables would result in an inordinately long computer run (greater than 10 hours on a CDC 7600), and an error would waste computer resources. Consequently, wing design was accomplished in a series of steps. First, the upper surface was designed one section at a time proceeding from the root to tip. Next, the lower surface is similarly designed.

The optimization is done using the desired viscous pressure distribution. Consequently, the design procedure produces the "fluid" wing geometry (that is, the desired solid wing geometry plus the boundary layer displacement thickness). The fluid wing is then analyzed and the entire process, or parts thereof, are repeated as required to produce the desired pressures.

d. Extraction of Solid Wing Geometry

The wing contours produced by the optimization include the boundary layer displacement thickness, δ^*. The solid wing geometry is found by subtracting δ^* from the computed wing contours at each of the design stations. A conventional 2-D integral boundary layer code[9] is used to compute δ^*.

e. Analysis of Optimized Wing

The performance of the optimized wing is investigated using both full potential and extended small disturbance viscous transonic codes. The solid wing geometry is used in these calculations.

3. CONFIGURATION DESIGN

The design procedure was used to design a new wing for the C-141/AC2 configuration. The goal of this study was to improve the wing aerodynamics and at the same time increase the wing thickness for the Mach = .80, C_L = .60 design condition. Increased wing thickness was sought to increase the fuel volume, and to reduce wing weight. The new design method will be shown to be a successful approach for obtaining the desired improvements in aerodynamic efficiency.

a. Starting Wing Selection

We chose a Lockheed transonic wing with which to start the design process. This wing was selected because the airfoils were systematically developed using state-of-the-art airfoil inverse and analysis transonic methods.

b. Interference Pressures

The use of an isolated wing code during numerical optimization is a key feature of the design method because its use minimizes computer resource requirements while yielding good predictions of upper surface pressures for high-wing configurations. The interference pressure perturbations are confined to the lower surface and are primarily due to the gear pod. Since the flow is subcritical on the lower surface, and since the interference pressures are small, they can be calculated using a subsonic panel method[10] which provides very good geometric resolution in the wing-body-gear pod area as shown in Figure 6.

Interference effects of the nacelle installation are determined by computations using a transonic wing-pylon-nacelle computer code.

c. Design Pressures

Target wing pressures were specified near the root, break, tip, and midway between the break and the tip. The upper surface pressures were selected to provide a weak shock wave on the outer panel near the 60% chord station. The root pressures were selected to minimize isobar unsweeping and to avoid large trailing edge pressure gradients which might result in the formation of a strong trailing edge shock wave.

d. Numerical Optimization

The numerical optimization procedure was used to determine the wing geometry which produces the desired wing pressures. The wing geometry was determined by specifying pressures at the four wing design stations shown in Figure 7. Linear lofting between geometry control stations was used to generate the wing surface. A constant normalized section wing carry-through was used.

Of note also in Figure 7 is the specification of tip pressures near the 85% span station. This choice was made because of the relative inaccuracy of computed results near the wing tip.

e. Extended Small Disturbance Design

The Lockheed extended small disburbance program was used in the initial wing design. The final wing pressures are compared with the target pressures in Figure 8. Also shown here is the agreement between target and computed pressures after the upper surface design of each span station. The agreement between target and computed pressures is fair.

Before continuing with the design process, the solid wing geometry was analyzed using viscous versions of both full potential[8] and extended small disturbance[7] codes. The results of these calculations are shown in Figure 9. On the premise that the FPE results are correct, these data show that the ESD code mispredicts the wing leading edge flow field, and this error causes complete disagreement between ESD and FPE results.

f. Full Potential Design

The failure of the ESD optimization to design accurately the wing leading edge made a second pass through the design procedure using a full potential equation analysis code necessary. The FPE optimization was done using the design variables and objective used in the ESD optimization. The target pressures were modified to produce a slightly weaker shock wave.

The resulting wing was analyzed using both the FPE and ESD viscous codes. The results are summarized in Figure 10. The codes produce results in good agreement with one another, indicating that ESD methods yield accurate results if the leading edge is properly designed. The wing pressures are quite satisfactory. There is no tendency for isobars to coalesce near the root trailing edge, nor is there a tendency for a leading edge shock wave to form. The desired mid-chord shock is weak (normal Mach number less than 1.16). Consequently, this FPE-designed wing was selected as the final C-141B/AC2 wing design.

4. WIND TUNNEL TEST

a. Test Facility

The design verification wind tunnel tests were conducted in the Lockheed-Georgia Compressible Flow Wind Tunnel (CFWT). The general arrangement of the CFWT is shown in Figure 11. The tunnel is of the blow-down type, exhausting directly to the atmosphere.

The semi-span configuration of the CFWT is shown in Figure 12 The model is mounted on a five-component balance located in the floor. A bleed duct is located 53.6 cm (21 in.) ahead of the balance centerline to remove the wind tunnel boundary layer. A more detailed description of the facility may be found in Reference 11.

b. Models

An existing .0188 scale C-141 semi-span model, Figure 13, was used to obtain baseline data. The new C-141B/AC2 wing, shown in Figure 14, was machined from a solid billet of 17 stainless steel.

c. Tests

The tests were conducted at a Reynolds number of 5 million over a Mach number range of 0.60 to 0.84, and an angle of attack range of -2 degrees to +4 degrees. The baseline C-141 model was tested in the semi-span wing configuration with fuselage and gear pod fairing. More extensive configurations including pylons and nacelles were tested for the C-141B/AC2 design.

5. DESIGN EVALUATION

a. Analysis of Test Data

The C-141B/AC2 design conditions and wing geometry are substantially different from the C-141. Consequently, a comparison of wing aerodynamics does not by itself provide a true measure of the effectiveness of the new wing. For example, a comparison of drag polars at the C-141B/AC2 design Mach number would not be meaningful because the C-141 was designed to cruise at .77 Mach, and its wing is well into drag rise at .80 Mach. Consequently, the efficiency of the design procedure is evaluated by comparison of complete airplane performance capabilities rather than by reference to incremental aerodynamic characteristics. To make these comparisons, flight aerodynamics for the C-141B/AC2 are extrapolated from wind tunnel data using the known C-141 flight characteristics as a calibration.

Because a reliable wall interference effects procedure for the Compressible Flow Wind Tunnel was not available, the analysis method adopted herein is based on a comparison of uncorrected measured and estimated drag differences for the two wing-fuselage-gear pod configurations. The drag estimation technique is known to agree well with C-141 flight experience.

A drag estimation at M - 0.70 was made for each configuration at the wind tunnel Reynolds number and then compared with the measured model drag. The resulting drag differences are shown in Figure 15. The variation with lift coefficient is identical for the two designs, and the C-141B/AC2 drag is 10 counts less than the C-141B drag. The actual drag of the C-141B full-scale aircraft is known from flight tests and is reproduced by the drag estimation method employed. Assuming that the drag increment is insensitive to Reynolds numbers, the full-scale drag of the C-141B/AC2 aircraft at M = 0.70 can be obtained by subtracting 10 counts from the full-scale estimation drag polar for the C-141B.

The next step in the drag analysis procedure was the determination of the drag rise Mach number and the compressibility drag increment. A direct comparison of the measured drag rise characteristics of the wing-fuselage-gear pod configurations at constant C_L is presented in Figure 16. The corresponding drag divergence Mach numbers, M_D, are shown as a function of lift coefficient in Figure 17. The target M_D value for the C-141B/AC2 design of $M = 0.80$ at $C_L = 0.60$ was not achieved. This results partly from the viscous uncambering of the cove region at the relatively low tunnel Reynolds number, and partly from the aeroelastic deformation of the model wing at the high dynamic pressures of the Compressible Flow Wind Tunnel. Reducing the full-scale design Mach number and lift coefficient to $M - 0.78$ and $C_L = 0.56$ in accordance with the measured data of Figure 17 nevertheless results in a highly satisfactory advanced technology C-141B/AC2 aircraft design.

b. Aircraft Performance

The payload-range performance predictions of the C-141B/AC2 based on wind tunnel data are compared to that of the C-141B and to the C-141B/AC2 target performance in Figure 18. Of note is the better than targeted ferry range of the C-141B/AC2 made possible to the thick wing resulting from the application of the new wing design method. The reduction in aircraft weights and fuel made possible by advanced technology are shown in Figure 19. The predicted gross weight reduction is 21%. This is 1% better than the target value of 20%. The predicted empty weight reduction is 24%, which is 4% better than the target value of 20%. The predicted block fuel decrease is 36% which is equal to the target value of 36%. Thus, with the exception of the .80 cruise Mach number, the study design objectives have been achieved.

c. Correlations

The experimental program was planned to provide an extensive data set particularly well-suited for code correlations. Specifically, pressure and force data are available for the following C-141B/AC2 configurations:

- Isolated Wing
- Wing + Pylon/Nacelle
- Wing + Fuselage
- Wing + Fuselage + Pylon/Nacelle
- Wing + Fuselage + Gear Pod
- Wing + Fuselage + Pylon/Nacelle + Gear Pod

Wind tunnel wall pressure data are available for use as far field boundary conditions for each of these configurations.

A viscous version of FLO22 developed by Henne was used to generate solutions for both the designed wing and the measured manufactured wind tunnel model. In the latter case, the wing spanwise twist was adjusted to simulate model deformation under load. Uncorrected test data were used in these early comparisons, and free-air far field boundary conditions were used in the calculations.

Isolated wing calculated and measured lift, stability, and drag polar curves are compared in Figures 20, 21, and 22, respectively, for .80 Mach. These comparisons show that the use of measured model ordinates and adjusted twist improve the agreement between calculated and measured wing aerodynamics. The difference between computed and test zero lift angle of attack is in part due to wind tunnel wall effects. The pitching moment discrepancy can be explained by examination of the chordwise pressure distributions.

Computed and measured C-141B/AC2 isolated wing pressures are compared in Figure 23. The use of measured ordinates and adjusted twist improves the correlation. However, the flow near the leading edge and in the lower surface cove region are mispredicted. The discrepancy on the cove pressures is clearly due to flow separation which was not modeled.

There are several possible reasons for the discrepancy near the leading edge, and we were not able to isolate any one reason in particular. The leading edge discrepancy is probably due to several factors acting together. The possibilities are: (1) Correlations were made to match total lift and not leading edge pressures, (2) Existence of a short separated region near the leading edge, (3) Transition strips which affect the readings of some of the leading edge pressure taps, (4) An actual twist distribution due to aerodynamic loading that is different from the predicted twist distribution, and (5) The small physical scale of the model which is conducive to leading edge irregularities.

Of particular note in the pressure distributions is the presence of a shock wave with an approximately constant sweep angle. This weak swept shock wave was specified in the target pressures used to design the wing. The shock wave behavior is fairly well predicted when the measured wing geometry with adjusted twist are used in the calculation.

6. CRITIQUE OF DESIGN PROCEDURES

This study has shown that numerical optimization provides a means to design wings which produce desired cruise pressure distributions and that the method can be incorporated within the framework of current aircraft design procedures. However, three areas have been identified where improvements to the current procedure can be made. These areas are:

1. Design variables
2. User expertise
3. Computation time

a. Design Variables

Sine deformation shape functions of the form $\sin^n(\pi x)$ provide the primary means of modifying the wing geometry to produce the desired pressures. The intent of these functions is to provide local geometric control. For example, the shape function $\sin^3\pi x$ produces maximum geometric change at the 50% chord station as shown in Figure 24. Also shown in that figure is the change in curvature produced by the shape function. Although the maximum curvature change occurs at 50% chord, there are two other locations of significant curvature change. Since curvature plays a dominant role in the development of the flow field, the non-localized curvature changes produced by the sine shape functions can cause undesired changes in the flow field and that introduces ambiguity in the optimization process.

A remedy is to use design variables based on the second derivative of the airfoil surface. Such shape functions not only localize the curvature variations, but also produce very smooth airfoils. Research is presently underway at Lockheed-Georgia and at the Ames Research Center, NASA, to develop efficient curvature-based design variables.

b. User Expertise

Engineers who are skilled aerodynamicists and who are familiar with numerical optimization are needed to successfully use optimization in aircraft design. This need exists because of (1) the requirement to accurately specify desirable pressure distributions which produce realistic wing geometries, and (2) difficulties encountered in selecting design shape functions which will produce the desired flow field modifications. The latter difficulty can be ameliorated by the use of curvature-based design variables.

Clearly, the difficulties encountered in the specification of desirable pressure is accentuated for multiple design point aircraft such as supersonic cruise/transonic maneuver fighters. For transport aircraft, consideration of wing weight and drag reduction must be balanced against one another. One possible solution to this problem is to conduct studies to identify sensible and desirable pressure distributions for different missions.

Another alternative is the use of design objectives based on aerodynamic forces and moments. For this approach to be successful, the accuracy of computed aerodynamic forces and moments, in particular drag, must be improved. Experience with current numerical aerodynamic methods, even in two dimensions, has shown that inaccuracies in drag calculations can make realistic and reliable numerical optimization difficult. If sufficiently consistent and accurate drag calculation techniques can be developed, then the use of design objectives based on integrated aerodynamic parameters would best take advantage of the capabilities offered by numerical optimization.

c. Computation Time

Between 5 and 10 hours of computation time on a CDC 7600-class computer are needed to perform a wing design using the subject numerical optimization scheme. These relatively large times are caused by the multitude of non-linear aerodynamic solutions required during the optimization process. The three obvious ways of reducing the computation times are (1) use more efficient computers, (2) use better solution algorithms, and (3) reduce the number of non-linear solutions.

The first two solutions are related and they involve the use of new algorithms such as approximate factorization schemes on new vector computers such as the CRAY-1 and the CDC Cyber 203. Significant research is being devoted to this task.

The third solution can be approached in at least two ways. One approach is to develop a versatile and reliable 3-D inverse transonic method in which the wing geometry is computed directly from the specified pressures. Such a method would require about the same computation time used in transonic flow analysis. A deficiency in this approach is that constraints are difficult to impose. Nevertheless, an inverse method could produce a wing that closely approaches an acceptable design. Numerical optimization could then be used for the final design refinements. The geometric changes might be expected to be less than for a complete optimization design, and fewer design variables might be required. Thus, the number of non-linear solutions needed in the optimization process should be reduced.

The second approach to reducing the number of non-linear solutions in fact involves the replacement of fine grid solutions with coarse grid results. To maintain accuracy, the coarse grid results are corrected to equivalent fine grid accuracy using Nixon's strained coordinate scheme[12]. The possibility of such an approach has already been explored by Lockheed-Georgia and Nielsen Engineering and Research scientists. In a proof of concept study, optimization, together with Nixon's strained coordinate scheme have been coupled to a 2-D transonic airfoil code. With this new scheme, computer time for airfoil design has been reduced by close to a factor of 5.

Implementation of a design procedure incorporating an inverse method with numerical optimization wing strained coordinates can be expected to reduce wing design computation time from the current 5 to 10 hour range to approximately 1 to 2 hours on a CDC 7600. By using an algorithm which takes advantage of new vector processing computers, computer-aided wing transonic aerodynamic design in less than ½ hour can be forecast.

7. CONCLUDING COMMENTS

We have developed a new transonic wing design method using the numerical optimization scheme. We have also shown that new computational methods offer a means for the aerodynamic design of wings with transonic performance superior to that which could be obtained using previous design techniques. The method is relatively easy to use, and it is compatible with established industry design procedures. By using the new method, a 40% to 50% reduction in the cost associated with wing cruise aerodynamic design is obtainable. By incorporating the strained coordinate scheme into the method, cost reductions should approach 75%. Additionally, adapting a strained coordinate version of the method to the new vector processing computers should make possible efficient wing design using less than ½ hour computation time.

SECTION III
FIGHTER DESIGN

1. FIGHTER CONFIGURATION SELECTION

The Configuration Development of Advanced Fighters (CDAF) dual-role concept [13] was selected for the fighter design methodology development. The criteria for its selection were: the ability to perform existing and future Air Force missions with significant performance improvements over existing aircraft, the incorporation of advanced technology and the potential to benefit from a new 3-D transonic design methodology. The CDAF configuration satisfies all these criteria.

a. Mission Performance

Several studies of the interaction of mission requirements, technology advancements and weapon system configurations have shown the need for supersonic dash rather than today's transonic cruise, through enemy airspace [14]. An objective of the Configuration Development of Advanced Fighters study was to derive, evaluate, analyze and test an advanced supersonic cruise fighter.

The "preferred concept" developed in the CDAF study is shown in Figure 25. The CDAF preferred concept is a dual-role vehicle developed for the fighter maneuvering role, emphasizing an air-to-air capability (Fighter) with designed-in flexibility for adequate air-to-ground performance (Penetrator). The key performance characteristics are:

	Fighter	Penetrator
Cruise Mach number	1.6	2.0
Subsonic radius (n mi)	100	365
Supersonic radius (n mi)	250	200
Weapon payload (lbs)	1000	4000
Installed avionics (lbs)	1375	1781
Takeoff ground roll (ft)	475	875
Landing ground roll (ft)	850	995
Sustained g's (M0.9/h 30K ft)	5.0	3.5
	(50% fuel)	(80% fuel)

The CDAF dual-role concept is a single place, flat-bottom, twin-engine, canard-wing aircraft configured for relaxed static stability. The aircraft was balanced 15% unstable at transonic speeds to minimize trim drag at transonic maneuver and supersonic flight conditions. The airframe architecture was tailored to meet the dual set of requirements demanded to efficiently perform in both air-to-air and air-to-ground missions. Smooth skin, variable camber leading and trailing edge flaps are incorporated on the wing. The chord ratio of the leading edge device increases toward the tip, while that of the trailing edge device increases toward the root. This system enables simultaneous variations of wing camber and twist to produce efficient contours throughout the flight envelope.

Wind tunnel data verify that the CDAF preferred concept represents a significant advancement in combining supersonic cruise and transonic maneuver capability. Figure 26 shows that transonic maneuver acceleration and supersonic cruise lift-to-drag ratio are both increased by 60% relative to current aircraft capability.

b. Advanced Technology Dependence

The impact of advanced technology in the CDAF preferred concept is illustrated in Figure 27. The figure shows the resulting takeoff gross weight (TOGW) increase when a technology component is "removed" from the configuration. A "conventional concept" cannot perform the CDAF design mission. When all of the advanced technologies are removed, the aircraft weight estimates show the fuel needed always exceeds the fuel available and the TOGW calculation diverges. The incorporation of advanced technology in the CDAF preferred concept is crucial to obtaining adequate performance for a supersonic cruise air combat mission.

c. Design Methodology Benefit

The maximum benefits of a transonic design methodology result when the most challenging performance goals are pursued. Maximum transonic maneuver performance for a supersonic aircraft represents the challenge. This cannot be considered simply as enhancement of a contemporary air combat fighter. Transonic maneuver requirements call for a relatively low wing loading and a moderately swept, high aspect ratio wing while supersonic cruise efficiency demands a relatively high wing loading and a thin, highly swept, low aspect ratio wing. These requirements dictate the most advanced transonic variable camber wing/airfoil technology available to resolve this "conflict". Maneuver wing design technology is the major design driver to minimize the spanwise varying airfoils and unique variable camber requirements if it is to meld good supersonic cruise performance with outstanding maneuvering capability. The primary aerodynamic need is to develop 3-D transonic design procedures to handle this nonuniform geometry.

2. SELECTION AND DEVELOPMENT OF METHODS

The key element of the design methodology is a 3-D transonic analysis code combined with numerical optimization. A new wing-body-canard transonic analysis capability was developed. Numerical optimization was chosen as part of the design methodology because it provides the greatest flexibility of design problem definition and analysis code selection. Numerous 2-D and 3-D applications have demonstrated the advantages of this approach.

a. Analysis Code Development

The wing-body analysis code of Boppe [15] was selected as the base upon which to develop a wing-body-canard analysis code. The code uses vertical line relaxation to solve a modified small disturbance equation in an "embedded grid" system. A pilot wing-canard analysis capability was demonstrated in Reference [16]. Figure 28 illustrates the embedded grid system for a wing-body-canard combination. The major modifications to the code were global mesh transformations for wing-canard planforms and provisions in the flow field solution to allow two lifting surfaces and their accompanying wakes. The flexibility of the nested mesh technique for configuration analysis is demonstrated in Reference [17].

The code analysis capability was evaluated with wind tunnel data for the CDAF configuration. Figure 29 shows results for three camber shapes. The amount of variable camber increase from the supersonic cruise (least camber) through transonic cruise to transonic maneuver (most camber). The code does not model the nacelles or vertical tail which are present in the data. Thirty counts of drag have been added to the analysis results. The computational mesh places fifteen analysis stations on the wing, eight analysis stations on the canard with eighty streamwise points on each airfoil section. Viscous effects are included with an infinite yawed wing boundary layer calculation at each analysis station. A typical computation requires approximately eleven minutes CPU time on a CDC 7600. A representative comparison of predicted and measured wing pressures is shown in Figure 30.

Comparisons of predicted wing pressure changes due to the canard on the CDAF supersonic cruise wing at Mach 0.9 are shown in Figure 31. Agreement between the predictions and data is good. Note that the change in pressures is significant only near the leading edge. This cannot be properly simulated with a simple local incidence change as it is sometimes done with a wing-body analysis code to approximate the canard effect on the wing.

The wing-body-canard analysis code was coupled with the COPES and CONMIN routines of Vanderplaats [18,6]. The COPES code is a control program that connects the numerical optimization code CONMIN with the aerodynamic analysis code. The resulting computer code was named PANDORA--Preliminary Automated Numerical Design Of Realistic Aircraft. The structure of the PANDORA code allows the numerical optimization to be coupled to any analysis code. Several "analysis" codes could be used together to provide information for the optimization. This information might be supersonic performance, TOGW changes or mechanical system sizing estimates. The available computer resources represent the only limit of complexity.

b. Design Procedure Development

Figure 32 illustrates the design procedure. The procedure defines a general systematic approach for any design problem that incorporates a transonic performance requirement. If the labels "transonic performance" and "non-transonic" were replaced with "design point" and "off-design", respectively, in Figure 32 then the design procedure can be applied to any aircraft mission performance design problem.

The design begins with a "conventional" wing design tailored to the particular requirements and philosophies of the specific configuration. Typically this is done using 2-D transonic and 3-D linear (subsonic and supersonic) computer codes. Then numerical optimization with a 3-D transonic code is used to refine the baseline wing geometry.

The numerical optimization requires the choice of design variables and optimization criteria. The key design variables control functions that modify the wing geometry. The optimization criteria consist of an objective function and constraints. The numerical optimization seeks to reduce the objective function (such as structural weight or aircraft drag). The constraints are conditions on the design (possibly none) that must be satisfied. Examples would be minimum fuel volume, maximum landing speed or minimum aircraft lift. The analysis code(s) evaluate the objective function and constraints for each design variable modifications made by the optimization code.

Two classes of design functions are typical: piecewise wing section ordinate functions and complete wing section shape functions. Examples from 2-D applications can be found in References [19] and [20]. For transonic maneuver, the optimization criteria are minimum drag with constrained lift and pitching moment. The more appropriate criteria would be maximum trimmed lift with constrained drag (i.e., the available thrust). Other equivalent criteria could be used.

If the criteria that determine the "best" configuration can all be evaluated with the 3-D transonic code, PANDORA can provide a self-sufficient design optimization. The particular constraints for a design optimization need be determined for the specific configuration (with its mission) that is being designed. Some constraints can be very simple, such as (mechanical) limits on the device deflections. These can be easily incorporated into the design variables and optimization function.

The design of realistic aircraft always involves a mission that includes non-transonic performance. Examples of non-transonic performance requirements are maximum lowspeed lift, supersonic cruise and supersonic maneuver. The transonic performance improvement may penalize the non-transonic performance. If so, the optimization function need be modified to include a "penalty factor" for the non-transonic performance penalty. Alternatively, the design variables may be modified to avoid or reduce the non-transonic performance penalty.

These modifications are determined external to the transonic analysis/optimization code. The implementation of these modifications requires quantified numerical formulas. Typically the change in estimated takeoff gross weight (TOGW) is used to quantify the trade between transonic and non-transonic performance. Then the "optimized" transonic performance with "satisfactory" non-transonic performance will be that which minimizes the aircraft TOGW while satisfying all the mission performance requirements.

3. CONFIGURATION DESIGN AND WIND TUNNEL TEST

The configuration design provides a detailed demonstration and evaluation of the transonic design methodology. As applied to the CDAF configuration, the design goal was to reduce the takeoff gross weight by minimizing transonic maneuver drag while maintaining adequate supersonic performance. The wind tunnel test of the resulting geometries provides the data necessary to verify the analysis/optimization capability of the PANDORA code.

a. Baseline Geometry Analysis

The baseline geometry used as a starting point for this effort was designed using supersonic 3-D codes [21,22]. The wing geometries for transonic cruise and maneuver were designed using subsonic codes [23,24] and prior wind tunnel experience from a similar configuration [25,26]. At the transonic maneuver conditions (Mach=0.9, C_L=0.7) both analysis and test data showed flow separation beyond the modeling capability of the code. A lower lift coefficient (C_L=0.5) was used as the design point for the numerical optimization in order to reduce the extent of flow separation.

In order to reduce the computer time needed for the optimization, the analysis model was simplified. The boundary layer modeling was deleted (i.e., an inviscid flowfield analysis was used) and the canard was eliminated from the configuration to be optimized. Code analysis of the baseline geometry showed little impact of these simplifications. The canard influence was confined to the forward part of the wing root region which is an area that was to remain fixed during the optimization. In general, the canard and viscous effects could be included in the optimization. A third step taken to reduce computing time was to reduce the number of mesh points in the flowfield analysis.

b. Optimization Function Definition

For aircraft design, the optimization function is that result of the aerodynamic analysis used to determine a "better" configuration. As applied to the CDAF configuration, the wing box geometry was not changed by the optmization procedure. With the wing box geometry held fixed, the technique of "optimizing" for a target pressure distribution does not provide a general method to determine the best transonic performance. The transonic performance itself need be the criteria for determining the optimum design. The usual optimization function for the CDAF design was to reduce the drag, subject to the inequality constraints of not decreasing the lift or pitching moment (a decreased pitching moment would be more nose down).

c. Design Variable Definition

Examples from earlier airfoil aerodynamic optimizations used two types of design functions: piecewise polynomial shape functions [19] and complete wing section shape functions [20]. Two design approaches, corresponding to these two types of design functions were used.

Initially, a "camber" approach was used--the design variables were a mathematical representation of the variable camber device geometry. The variable camber segmentation is shown in Figure 33. Figure 34 illustrates the equation relating a design variable V(N) to a "device deflection" Z(N). The equations used represent the classical solution of a deflected, cantilevered beam. Small deflections are assumed, so that changes in the device arc length are ignored. This choice of design variables does not penalize the supersonic performance since the wing geometry can return to the supersonic cruise shape. (There were no mechanical system limits imposed on the deflections.) Additional design variables can be incorporated by subdividing the variable camber segments.

Originally, eleven design variables were used to "deflect" the wing devices as sketched in Figure 35. A twelfth design variable was used to change the angle of attack. Later, sixteen design variables were used by subdividing four of the original camber segments. The four most outboard segments were subdivided first (segments 8-11 in Figure 35) and then, separately, the four most inboard segments were subdivided (segments 1-4 in Figure 35). The starting wing geometry was the transonic maneuver shape of the baseline configuration.

The second approach was a wing section "shape" approach. At each of the five defining span stations in Figure 35, two complete wing section shapes were specified and the optimization determined the best linear combination of the two shapes. The design variable at each span station represents the weighting factor for combining the two shapes, as shown in Figure 36. One of the sets of shapes used was the baseline transonic cruise wing sections. The other set of shapes was the transonic maneuver wing sections with reduced trailing edge deflections at the two most inboard stations. The sections have a common wing box shape, so that their combination results in geometry changes only where device deflection occurs. Requiring only six design variables, the shape approach is much simpler than the camber approach.

d. Transonic Performance Optimization

Initial results using the camber approach with twelve design variables showed a calculated drag reduction of more than thirty counts (for the inviscid, thinned-grid analysis). Total CPU time was less than two hours. Subsequent optimization runs with sixteen design variables produced no significant additional drag reduction.

Three additional runs were made with the sixteen design variables. Two of these runs redefined the optimization criteria and the third perturbed the starting values of the design variables. The two additional optimization criteria were to minimize the square root of the drag and to maximize lift with a drag constraint of not more than the starting value. No significant change to the resulting design variables occurred.

The final result of all the optimization runs with the camber approach was a predicted drag reduction of more than forty counts, ignoring any changes in lift and moment (approximately -.01 and +.01, respectively). Total CPU time for all the optimization runs was less than four hours. The trailing edge location at span stations 0.544 and 0.816 moved downward, while that of the theoretical tip moved upward. A "full-grid" wing-body viscous analysis at the nominal design conditions showed the lift coefficient to be approximately .04 less than the starting value. Matching the starting lift value, the estimated drag reduction was less than six counts. With the trim drag reduction due to less negative pitching moment, the total expected drag reduction was approximately fifteen counts.

The second optimization approach used significant less computer time because of the fewer number of design variables. Two optimization runs reduced the predicted drag value by more than twenty counts. A third run to minimize the square root of the drag produced no significant changes in two optimization iterations. Total CPU time was less than two hours.

Relative to the baseline transonic maneuver geometry, the predicted drag reduction for the shape approach was essentially the same as the camber approach (more than forty counts). Changes in lift and moment were also the same. The trailing edge location of the two most inboard devices was raised, while that of the third (span station .544) was lowered. The leading edge was moved downward at all three span stations. Again, a "full-grid", viscous, wing-body analysis indicated a drag reduction of less than six counts at the starting value of lift. With the expected trim drag change, the total drag reduction was again approximately fifteen counts.

The problem of local and global optimums in an optimization problem is demonstrated by the results of the two approaches. The two "optimum" device deflections moved in opposite directions at span stations .544 and 1.0. The predicted performance is the same, which may or may not be the "true" optimum. There is little doubt of the non-uniqueness of a configuration design problem. The design space must include the true optimum if it is to be found with numerical optimization. If several optimums exist, then several different design variable or different starting solutions are needed to find the other optimums.

e. <u>Wind Tunnel Test</u>

The two wing geometries designed with the PANDORA code were tested in the Arnold Engineering Development Center 16T Propulsion Wind Tunnel in April 1980 [27]. The CDAF configuration had been tested previously in the 16T tunnel in April and November 1979 [28,29]. For all tests, the Reynolds number was 3.0 million per foot for subsonic Mach numbers and 1.5 million per foot for supersonic Mach numbers. Test Mach numbers were varied from 0.6 to 1.2. The fifteenth scale model had a mean aerodynamic chord of 11.3 inches, and was instrumented with a six component balance and ninety six pressure taps distributed on the wing and canard. The wind tunnel model is shown in Figure 37. The April 1980 test included canard on and off and nacelle on and off pressure data to provide a data base for both current and future code verification.

An "alternate maneuver" wing geometry was tested in November 1979. The alternate maneuver geometry represents a variable camber shape between the transonic cruise and original transonic maneuver. The model parts for the alternate maneuver geometry were made from the original transonic maneuver model parts. Thus, the baseline geometry used to start the optimization was not available for the test in April. The alternate maneuver geometry was tested with the PANDORA developed geometries to provide a test repeat reference.

4. AERO DATA EVALUATION

Representative test results for lift and moment at Mach 0.9 are summarized in Figure 38. The wing-body pitching moment non-linearities indicate strong wing tip flow separation. This was confirmed by oil flow visualizations. Wing-body-canard lift and moment at Mach 0.9 are included in the figure. Again the pitching moment non-linearities indicate strong viscous effects: wing tip separation and vortex flow on the canard.

Test results for wing-body lift and drag are compared to each other and code predictions in Figure 39. The code does not model the vertical tail which is present in the data and ten counts of drag have been added to the analysis results. The predicted drag levels agree with the data within twenty-five counts. The data show that the two PANDORA shapes have essentially the same performance as predicted by the optimization runs.

Lift and drag data and predictions for wing-body-canard configurations are shown in Figure 40. The relative performance of the two tested configurations is the same as in Figure 39. Code predictions are within twenty-five counts of the data. Again, the vertical tail is present in the data, but not in the analysis. Thirty counts of drag have been added to the analysis results.

The nominal lift coefficient for the numerical optimization is C_L=0.5. Ignoring trim drag, the data for the full configurations show no drag reduction at the design lift. The pitching moment change was +.032 for both PANDORA shapes, relative to the baseline. The trim drag reductions are fifteen and thirteen counts for the first and second shapes respectively. The moment change is greater than what was predicted. The resulting total drag reductions, however, are very close to what was predicted.

In addition to flow separation, the flow near the wing tip is quite severe for potential flow analysis (e.g., Figure 30). Data show local Mach numbers in excess of 1.7. The limit of potential flow analysis is generally considered to be about Mach number 1.3. A more complete flow equation (e.g., Euler, Navier-Stokes) need be used to accurately predict the flow details.

The actual maneuver point occurs at approximately eight degrees angle of attack. Both local flow speeds and viscous effects are too severe for proper potential flow analysis. Thus, the numerical optimization was applied to a lower angle of attack.

Performance improvements at C_L=0.5 did not improve the performance at the actual maneuver point (C_L=0.7). Thus, the mission performance (or takeoff gross weight) is unaffected. The performance improvement obtained at the optimization design point does represent a validation of the design procedure methodology.

5. EVALUATION OF DESIGNS

The application of the ATT design methodology to the CDAF configuration took approximately four hours of CDC 7600 CPU time for the camber approach and less than three hours CPU time for the shape approach. Nearly all of the geometry changes occured in the first two optimization runs, using approximately two hours of CPU time for each approach. Calendar time for the two methodology applications was approximately one month. Test results showed the resulting performance improvement to be a drag reduction of fifteen counts.

Thus, one design methodology application would use approximately two hours of CPU time and two weeks of calendar time (for an approach that has no non-transonic performance penalties). Four hours of CPU time would be adequate for a general, multi-pont design application. This would compare to a "manual" design approach that relies on wind tunnel data. A manual design requires wind tunnel data to "calculate" an improved wing geometry. The resulting performance improvement can only be estimated based on previously tested wing geometries.

The above comparison allows a large range of claims about the design methodology benefits. A detailed, quantified cost comparison can not be made since labor, testing and computer costs vary substantially. Ignoring calendar time, the only significant cost of the automated design methodology is the computer resources. The cost of the manual approach need include some of the expense of acquiring the baseline performance data. The manual approach need also have the additional wind tunnel testing of the new geometry to quantify its performance. A manual approach can never conclude that a geometry is optimum without additional testing. Such a conclusion is the end result of numerical optimization. The automated design methodology provides its own baseline performance "data" and quantifies the expected performance improvements.

The cost of fabricating and testing one additional wing geometry is twenty to forty thousand dollars. The lower number is more than the cost of four hours of CDC 7600 computer time. If the code results can be used to eliminate the need to test an additional wing geometry, then the cost savings equal, or exceed, the computer costs. Another requirement of the manual design approach is the time between the original and subsequent wind tunnel tests. It is clear that the automated design methodology can provide reduced development time or costs for the design of advanced fighter configurations.

The potential flow transonic analysis limited the design point lift to a value below the actual maneuver design point. A manual approach has no such limitation because it uses wind tunnel data. The ability of the automated design procedure to produce a performance improvement was demonstrated by the measured drag reduction at the optimization design lift. The crucial requirement to obtain a significant impact on the mission performance is the ability of the transonic analysis to accurately analyze the design point conditions.

A drag reduction of fifteen counts is very small compared to the total drag at transonic maneuver conditions. In fact, a thirty count drag reduction was felt to be the minimum for a "significant" impact on the configuration. However, if the computational analysis can be used to confidently predict that a given wing geometry is the "optimum," then considerable design time and costs can be saved. Several CPU hours is a small expense compared to that of the design, fabrication, and test of an additional set of wing devices. As improvements in both computer and code capability continue to be made, numerical methods become more cost effective. If existing faster computers are considered, CPU time reductions of a factor of two to five are obtainable. Such a reduction would allow more accurate analysis (e.g., explicit viscous effects, greater density grids) and yet use considerably less CPU time than that reported here.

This study was limited to one particular design application for a supersonic cruise transonic fighter. As discussed in previous sections, the final design problem for numerical optimization was a small part of the complete configuration design problem. Approximations made during the design problem numerical modeling (e.g., trim drag benefits, viscous effects) reduced the measured performance improvements from that predicted by the optimization runs. The benefits of numerical optimization will increase as the accuracy and completeness of the numerical simulation of the design problem increases.

6. FINAL DESIGN PROCEDURE

The experience of applying the original design procedure to the CDAF configuration led to several conclusions regarding the design methodology application. The design methodology is most effective when the numerical optimization is used most efficiently. Two key items can be identified for this: definition of the optimization function and design variables; and adequate analysis code accuracy.

All of the significant performance improvements occurred in the first two optimization iterations. The additional runs which made slight changes in the optimization function were not worthwhile. Changing the starting geometry or the design variables is more effective. Minimizing the drag or its square root (with a lift constraint) are the same optimization problem. Maximizing the lift-to-drag ratio with a lift constraint is better.

During the optimization, the influence of the design variables is calculated for the gradient information. When identified, the less effective design variables should be eliminated. The use of wing section shapes can produce good results with relatively few design variables. Detailed geometry variations with the numerical optimization is appropriate when specific local aerodynamic characteristics need be modified. If a mechanical system is to be modeled, then the design variables may be pre-determined by the system mechanism or else be sufficiently detailed to simulate a proposed system. Such a case is as much an optimization of the mechanical system as it is the configuration aerodynamics.

The need for accurate transonic analysis in the numerical optimization is clear. Inaccuracies in the analysis produce errors in the gradient information used in the optimization search. Reduced mesh densities reduce the necessary computer time, but at the risk of unacceptable analysis errors. Each design application should evaluate the impact of reduced mesh densities with several code analysis runs. Although fifty streamwise points per airfoil chord were used for the CDAF design, eighty points per chord seem necessary. The spanwise reduction of the fine grid system (from fifteen stations on the exposed span to twelve) yields satisfactory results. Improvements in the analysis code efficiency reduce the necessary computer time without any decrease in the analysis accuracy. More advanced computers and solution algorithms will improve the computer time/accuracy trade off. For example, the analysis code in PANDORA has been made twenty percent more efficient in CPU time since the original design methodology application.

7. CONCLUSIONS

The results described here show both the benefits and hazards of numerical optimization for aerodynamic design. The numerical optimization will work best when both the flowfield analysis and numerical model of the design problem are accurate. Although greater computer resources are generally needed for more complex and accurate analysis, the cost of numerical optimization would still be less than that of additional wind tunnel testing. As both computer and analysis code capability increase, numerical optimization will take a greater role in aerodynamic design. For a variable camber wing geometry, evaluation of different mechanical systems is well suited for numerical optimization. Numerical optimization can be used to evaluate the resulting performance of mechanical systems with different complexity, cost or weight. The aerodynamic designer can best use numerical optimization by running two or three iterations for a variety of geometries and starting conditions. The numerical optimization will conduct a systematic parametric evaluation using the flowfield analysis as if it were a wind tunnel. The computer can be used to compare many different configurations over several days time at a small fraction of the time and cost that would be needed to conduct a wind tunnel test.

References

1. Blackwell, J. A.: "An Empirical Correction for Wind Tunnel Wall Blockage in Two-Dimensional Transonic Flow." AIAA Paper No. 78-806, April 1978.

2. Blackwell, J. A.: "Scale Effects on Supercritical Airfoils." 11th Congress of the ICAS, Lisbon, Portugal, Sept. 10-16, 1978.

3. Hicks, R. M., and Henne, P. A.: "Wing Design by Numerical Optimization." AIAA Paper No. 77-1247, Aug. 1977.

4. Haney, H. P., Waggoner, E. G., and Ballhaus, W. F.: "Computational Transonic Wing Optimization Model." AIAA Paper No. 78-102, Jan. 1978.

5. Lores, M. E., Smith, P. R., and Hicks, R. M.: "Supercritical Wing Design Using Numerical Optimization and Comparisons with Experiment." AIAA Paper No. 79-0065, Jan. 1979.

6. Vanderplaats, G. N.: CONMIN-A Fortran Program Constrained Function Minimization-User's Manual. NASA TM X-62282, Aug. 1973.

7. Ballhaus, W. F., Bailey, F. R., and Frick, J.: "Improved Computational Treatment of Transonic Flow About Swept Wings." NASA CP-2001, Nov. 1976.

8. Jameson, A.: "Iterative Solution of Transonic Flows Over Airfoils and Wings." Comm. Pure Appl. Math., Vol. 27, 1974, pp. 283-309.

9. McNally, W. D.: "FORTRAN Program for Calculating Compressible Laminar and Turbulent Boundary Layers in Arbitrary Pressure Gradients," NASA TN D-5681, May 1970.

10. Hess, J. L.: "Calculation of Potential Flow About Arbitrary Three-Dimensional Lifting Bodies," McDonnell-Douglas Rept. No. MDC 15679-01, Oct. 1972.

11. Pounds, G. A., and Stanewsky, E.: "The Research Compressible Flow Facility, Part I - Design," Lockheed-Georgia Company ER-9219-1, 1967.

12. Nixon, D.: "Perturbation of a Discontinuous Transonic Flow," AIAA Paper No. 77-206, 1977.

13. "Configuration Development of Advanced Fighters," Final Technical Report, AFWAL-TR-80 3142, November 1980.

14. Riccioni, E. E. and Draper, A. C. (Conference Chairmen): "Design Conference Proceedings: Technology for Supersonic Cruise Military Aircraft, Vol I." AFFDL-TR-77-85, Vol I, Apr 76.

15. Boppe, C. W., "Transonic Flowfield Analysis for Wing-Fuselage Configurations," NASA Contractor Report 3243, May 1980.

16. Boppe, C. W., "Calculations of Transonic Wing Flows by Grid Embedding," AIAA Paper 77-207, January 1977.

17. Boppe, C. W., and Aidala, P. V., "Complex Configuration Analysis at Transonic Speeds," in Subsonic/Transonic Configuration Aerodynamics, AGARD CP-285, September 1980.

18. Vanderplaats, G. N., "COPES-FORTRAN Control Program for Engineering Synthesis," to be published as a Naval Postgraduate School Memorandum.

19. Vanderplaats, G. N., Hicks, R. M. and Murmann, E. M., "Applications of Numerical Optimization Techniques to Airfoil Design," NASA SP-347, Part II, 1975.

20. Vanderplaats, G. N. and Hicks, R. M., "Numerical Airfoil Optimization Using a Reduced Number of Design Coordinates" NASA TM X-73151, 1976.

21. Woodward, F. A., et. al., "Analysis and Design of Supersonic-Wing-Body Combinations, Including Flow Properties in the Near Field," NASA CR-73106, 1967.

22. Harris, R. V., "An Analysis and Correllation of Aircraft Wave Drag" NASA TM X-947, 1964.

23. Boppe, C. W., "A Computer Program for Calculating Subsonic Aerodynamics of Complex Wing-Body Configurations (A User's Guide)," Grumman Aerodynamics Technical Report No. 393-73-1, October 1973.

24. Mason, W. H., "Computation of Minimum Trimmed Drag Attainable on Complex Configurations and the Associated Design Spanloads," Grumman Memorandum EG-ARDYN-78-44, May 1978.

25. Meyer, R. C., Fields, W. D. "Configuration Development of a Supersonic Cruise Strike-Fighter," AIAA Paper 78-148, AIAA 16th Aerospace Sciences Meeting, Huntsville, Alabama, January 1978.

26. Hendrickson, R., Grossman, R., Sclafani, A. S. "Design Evolution of a Supersonic Cruise Strike Fighter," AIAA Paper 78-1452, AIAA Aircraft Systems and Technology Conference, Los Angeles, California, August 1978.

27. Spurlin, C. J., Test Report for AFWAL Optimal Transonic Configuration Fighter, Project No. P41T-G6, Test No. TF570, April 1980.

28. Spurlin, C. J., Test Report for AFFDL CDAF Configuration, Project No. P41T-B2, Test No. TF-534, April 1979.

29. MacLanahan, D. A., Jr., Test Report for AFFDL Advanced Survivable Aircraft Configuration, Project No. P41T-E0, Test No. TF-555, December 1979.

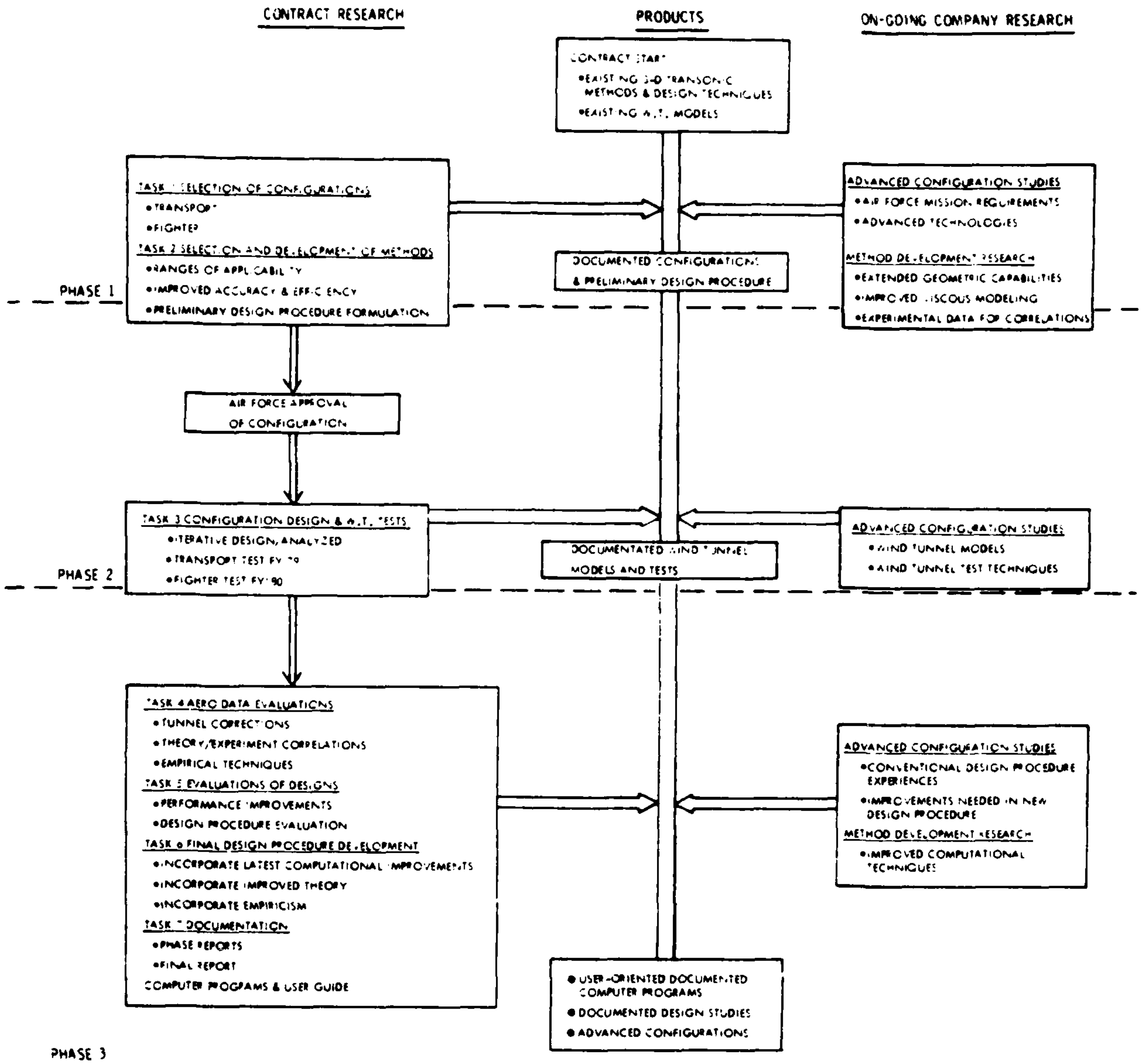

Figure 1. Program Plan

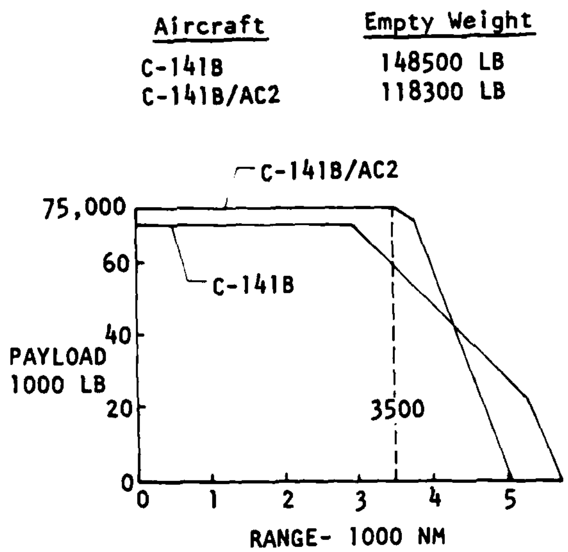

Figure 2. Targeted Performance

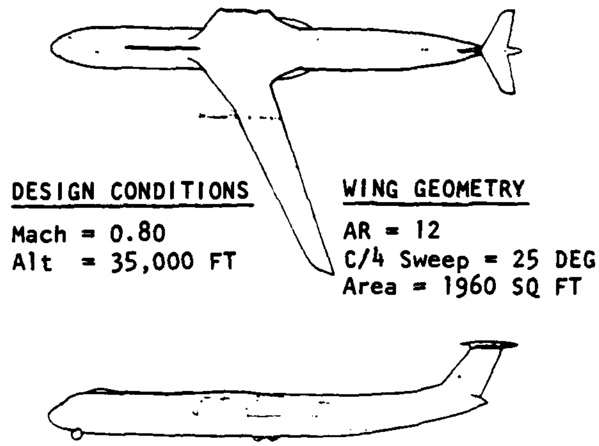

Figure 3. C-141B/AC2 General Configuration

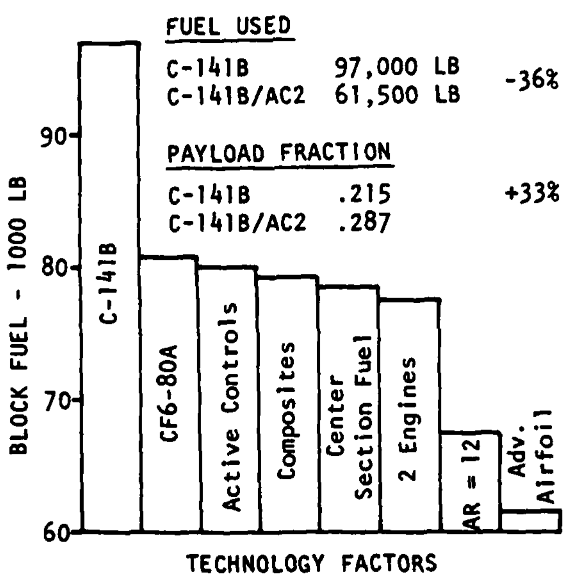

Figure 4. Technology Benefits

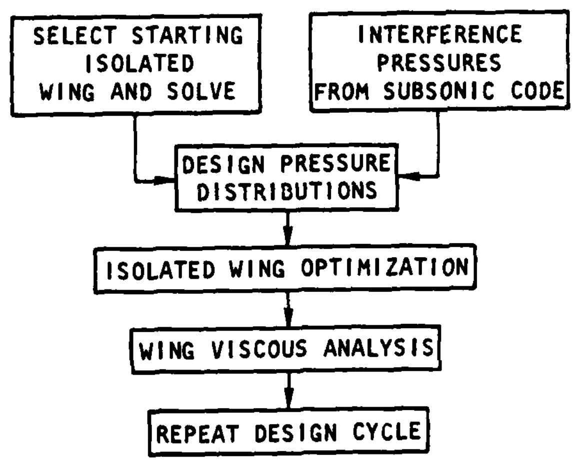

Figure 5. Design Procedure

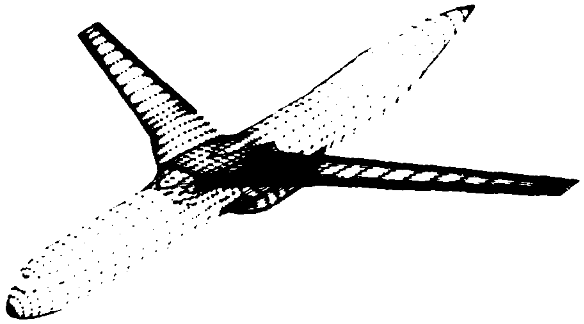

Figure 6. Subsonic Code Modeling

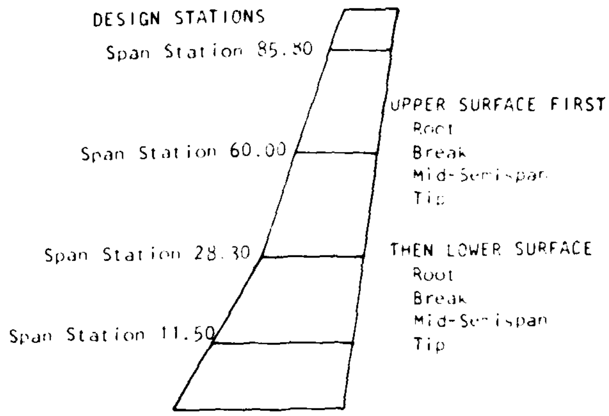

Figure 7. Wing Representation for Design

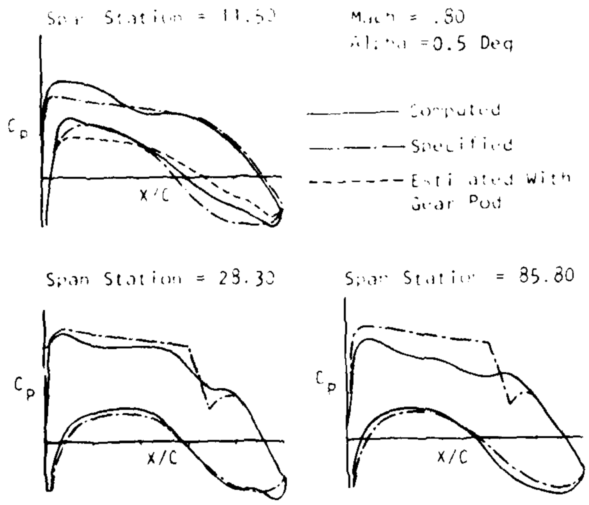

Figure 8. ESD Optimization Pressures

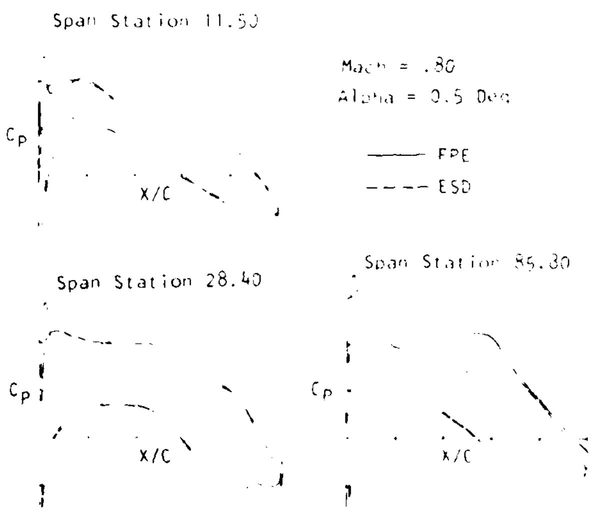

Figure 9. Analysis Of ESD Wing

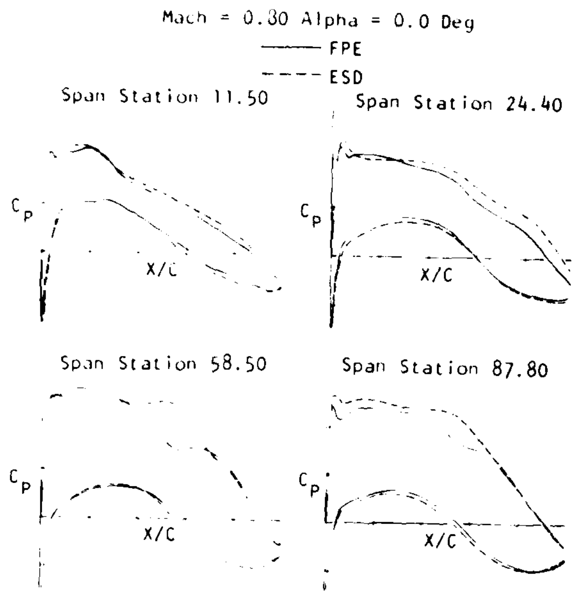

Figure 10. Analysis of FPE Wing

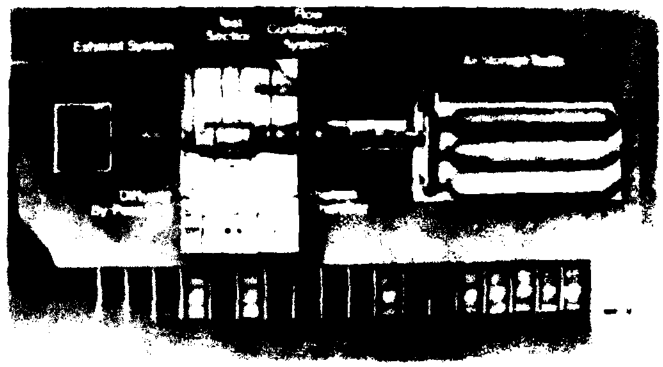

Figure 11. Lockheed-Georgia Compressible Flow Wind Tunnel

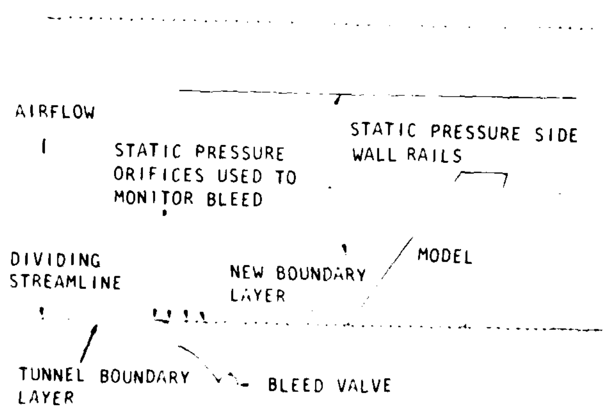

Figure 12. Semi-span Test Arrangement

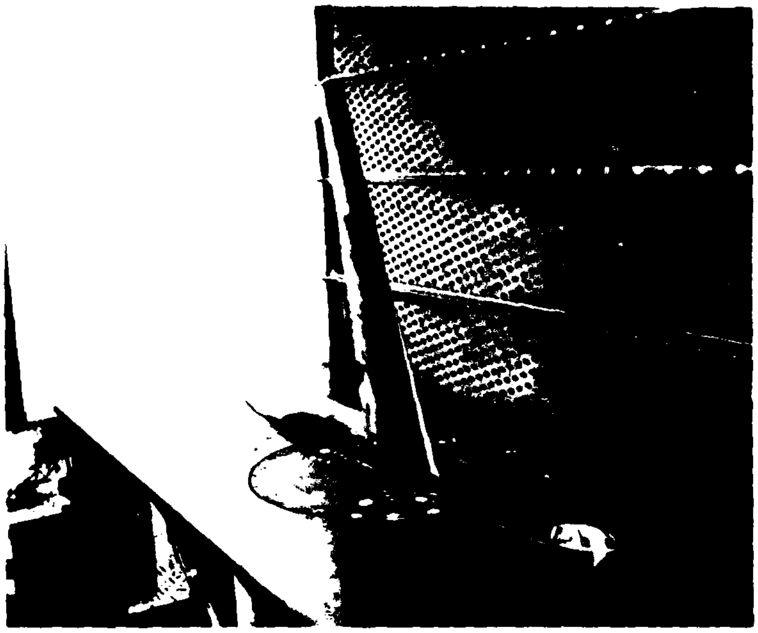

Figure 13. C-141B Model Installation

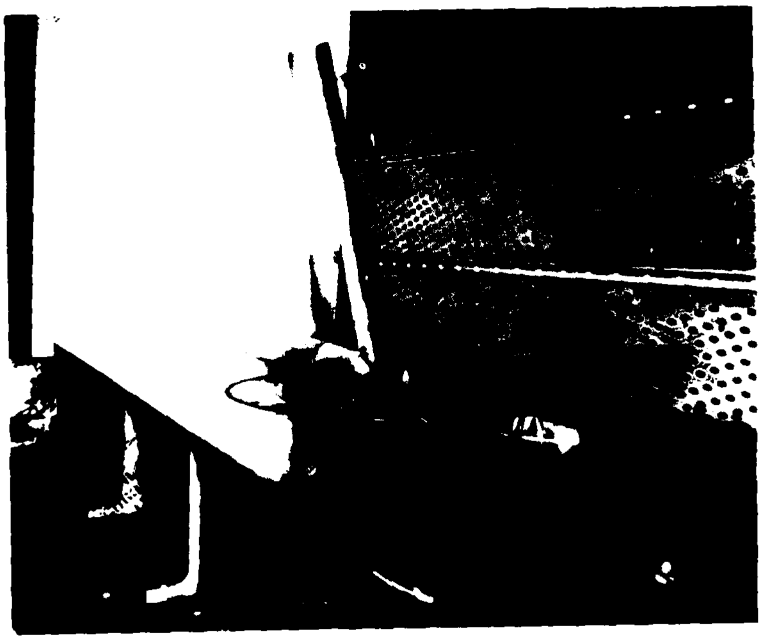

Figure 14. C-141B/AC2 Model Installation

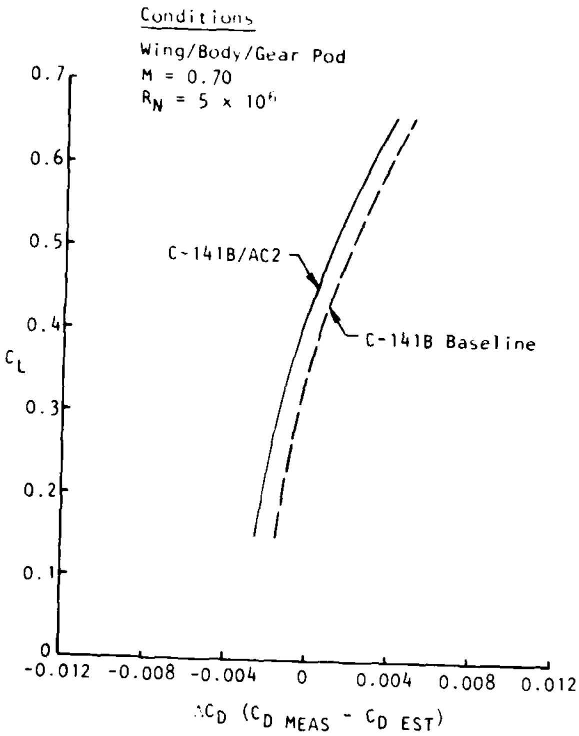

Figure 15. Comparison of Measured Model Drag With Estimates

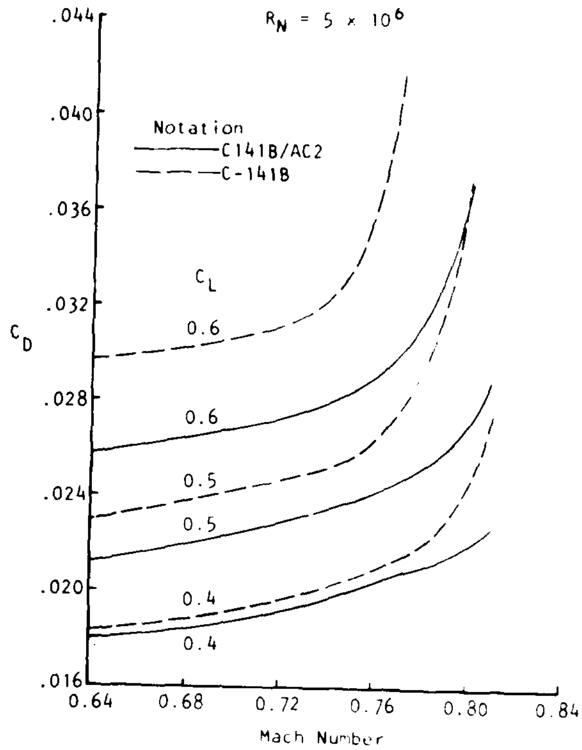

Figure 16. Measured Drag Rise Characteristics

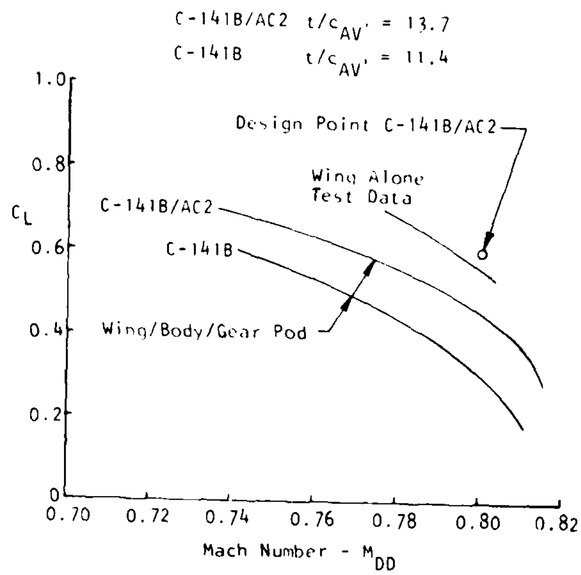

Figure 17. Measured Drag Divergence Mach Numbers

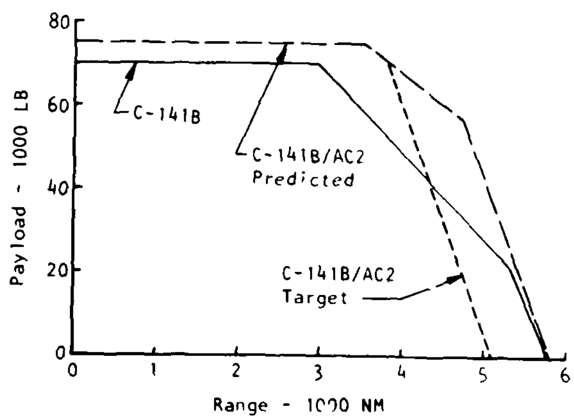

Figure 18. Payload-Range Performance

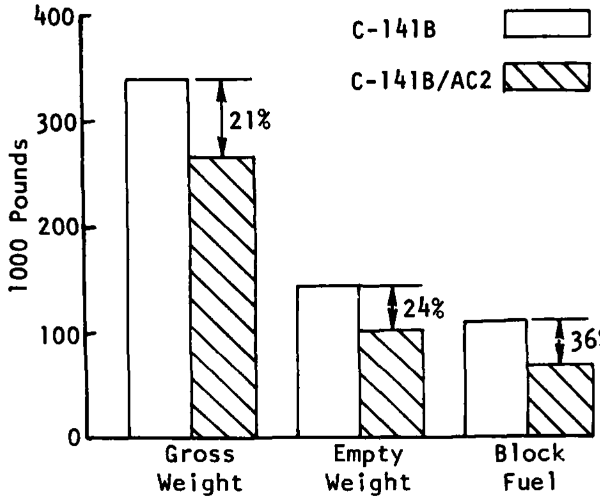

Figure 19. Summary of Aircraft Parameters

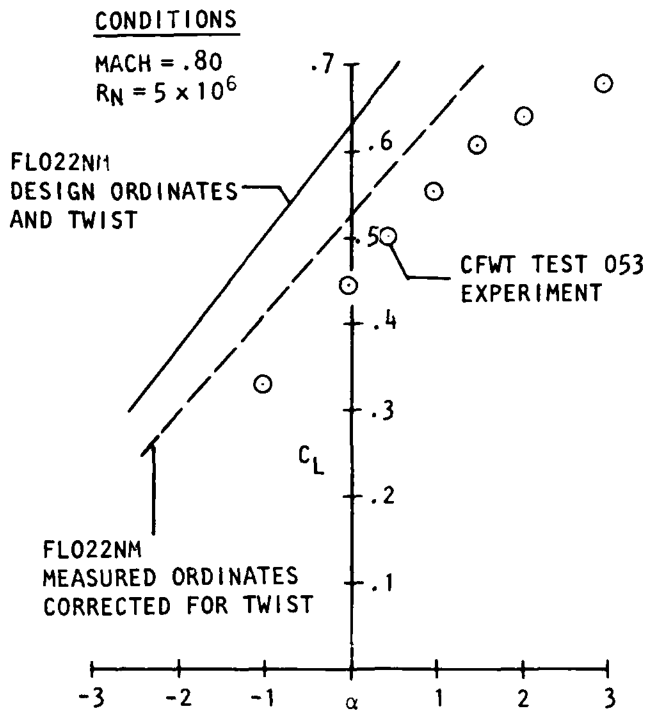

Figure 20. C-141B/AC2 Isolated Wing Measured and Computed Lift

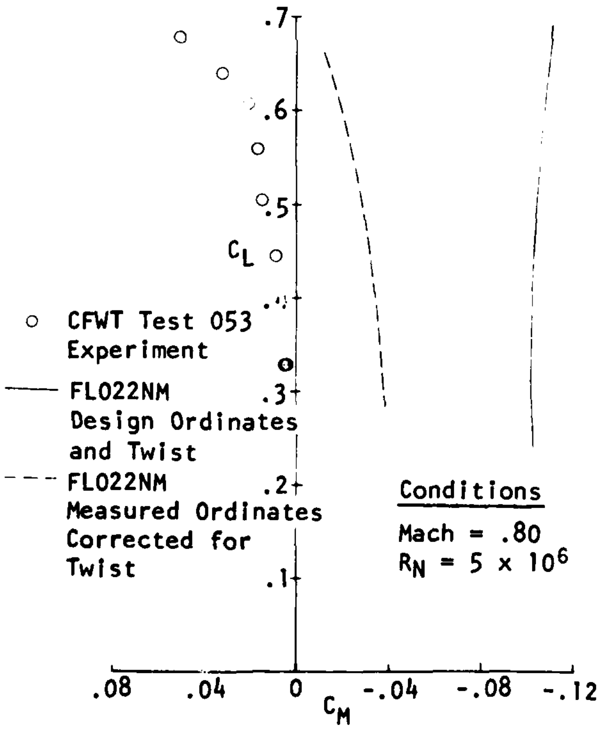

Figure 21. C-141B/AC2 Isolated Wing Measured and Computed Stability

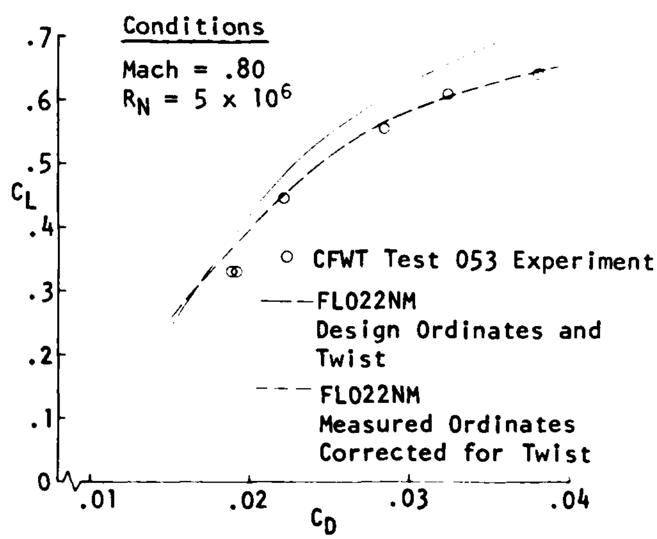

Figure 22. C-141B/AC2 Isolated Wing Measured and Computed Drag Polar

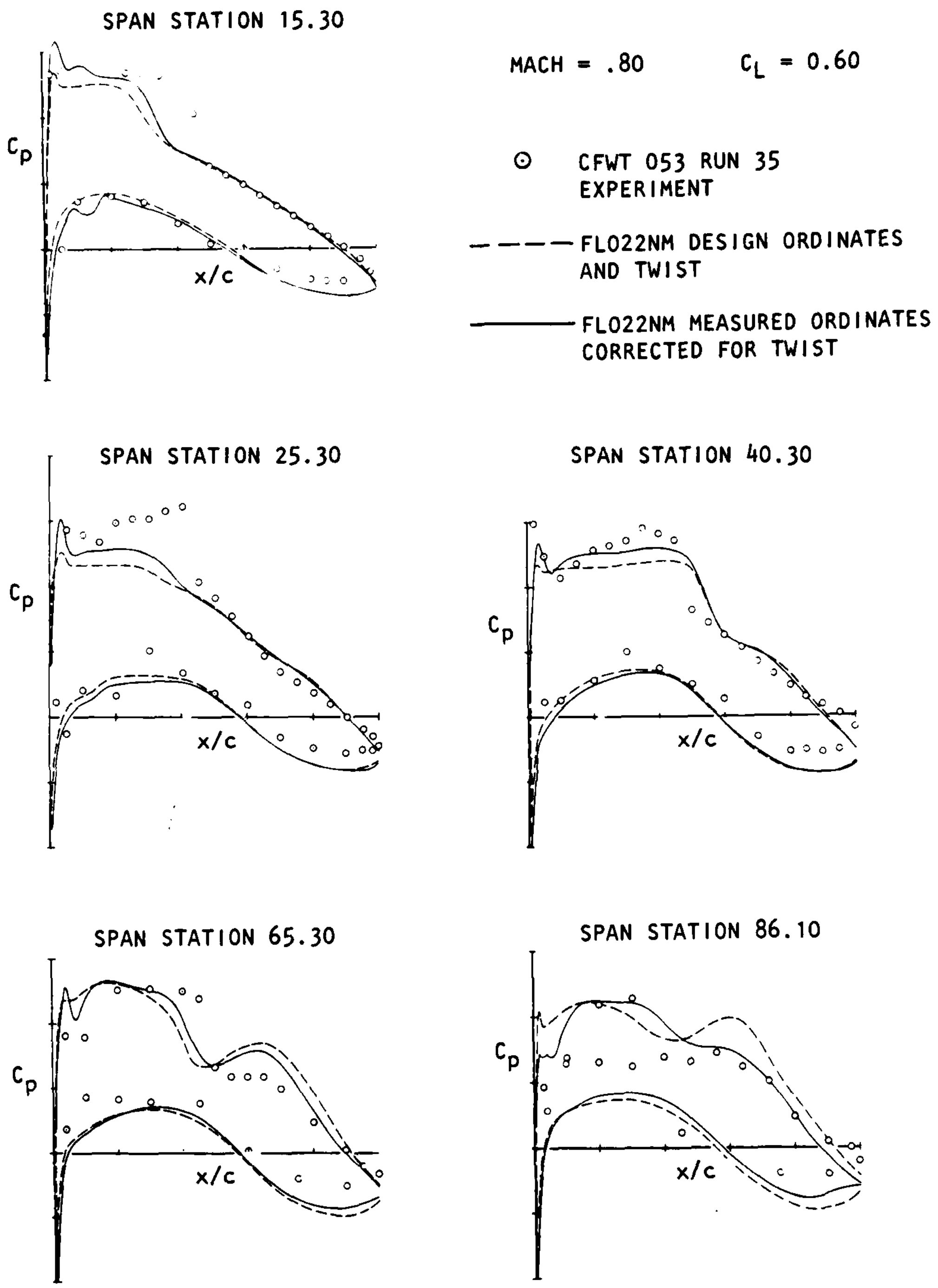

Figure 23. Measured and Computed C-141B/AC2 Isolated Wing Pressures

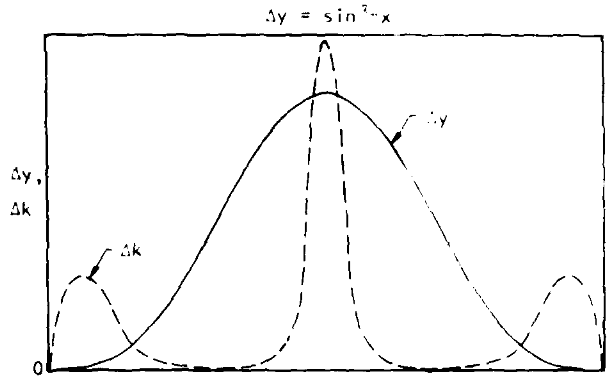

Figure 24. Airfoil Ordinate and Curvature Change

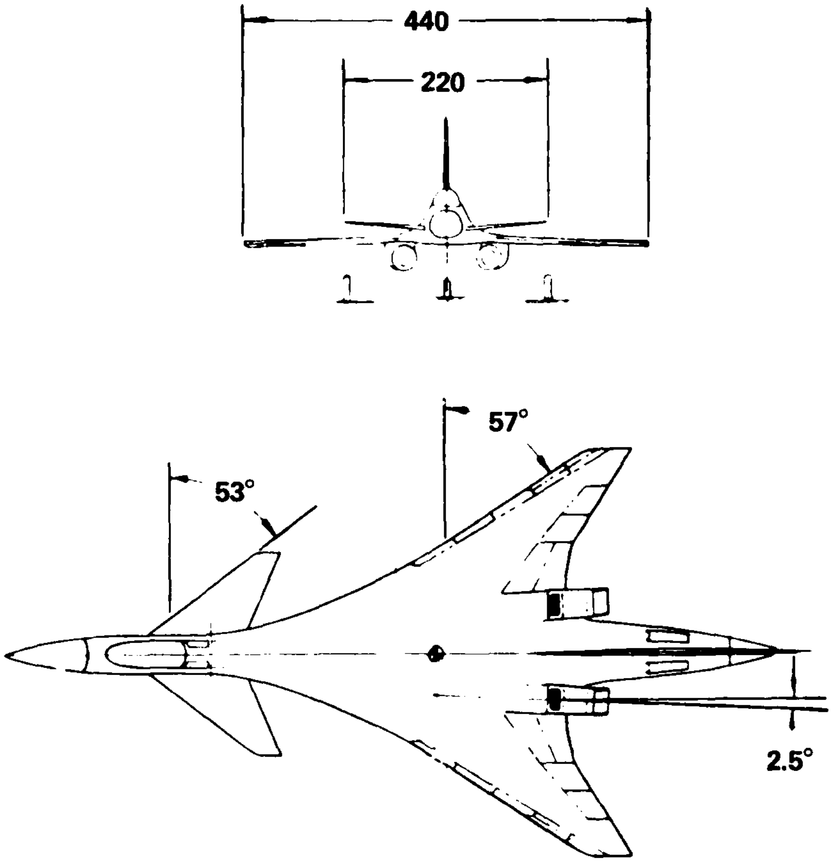

Figure 25. Fighter Design Configuration - CDAF Preferred Concept.

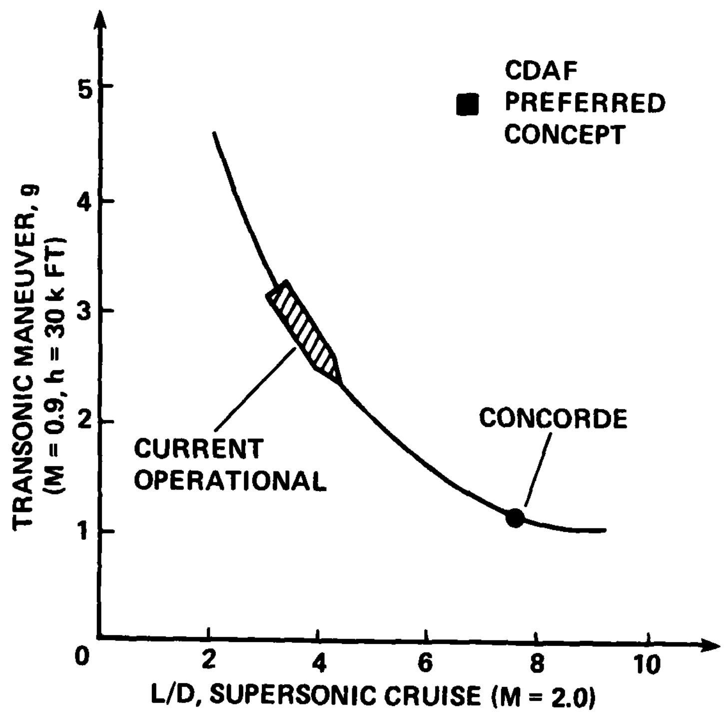

Figure 26. Comparison of Transonic Maneuver/Supersonic Cruise Performance of Current Aircraft and the CDAF Dual Role Concept.

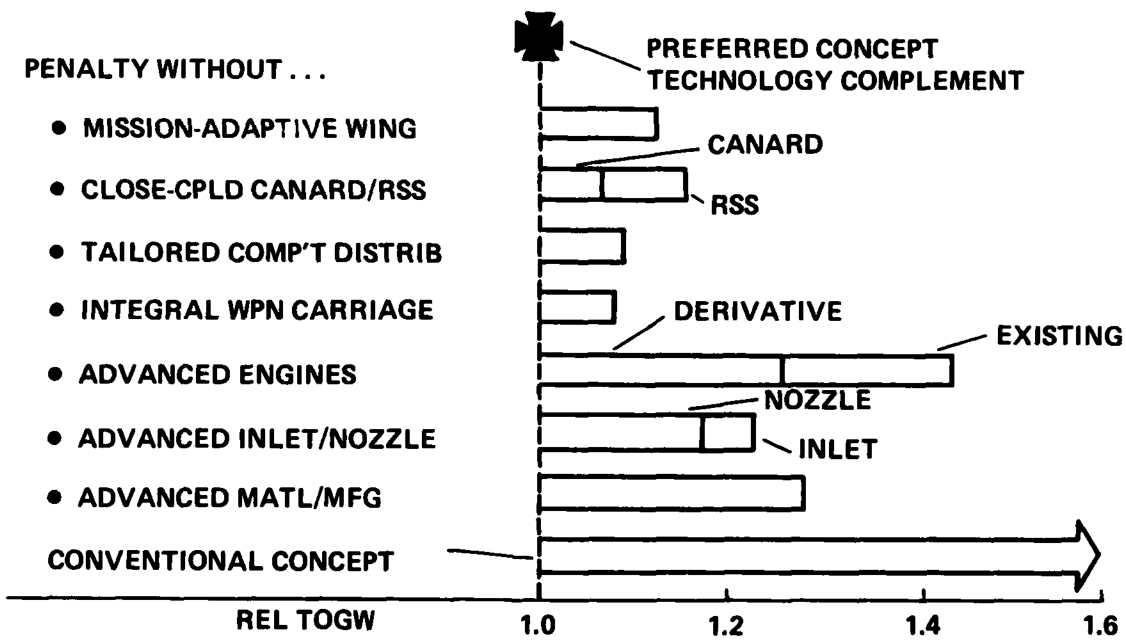

Figure 27. Advanced Technology Dependence of the CDAF Configuration.

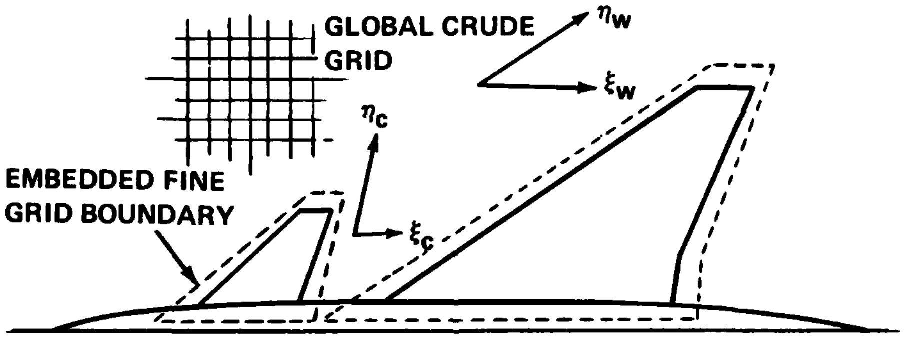

Figure 28. Embedded Grid System for a Wing-Body-Canard Configuration.

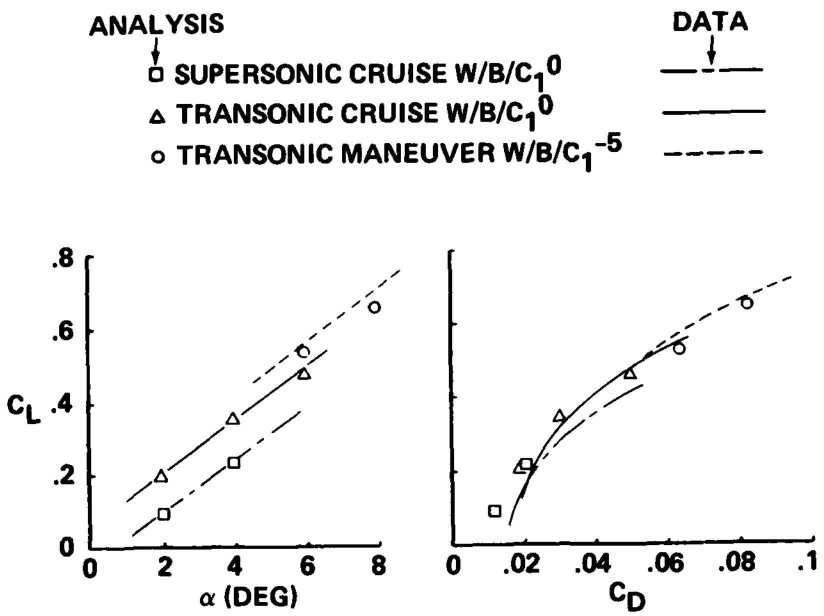

Figure 29. Wing-Body-Canard Lift and Drag, Data-Analysis Comparisons Mach 0.9

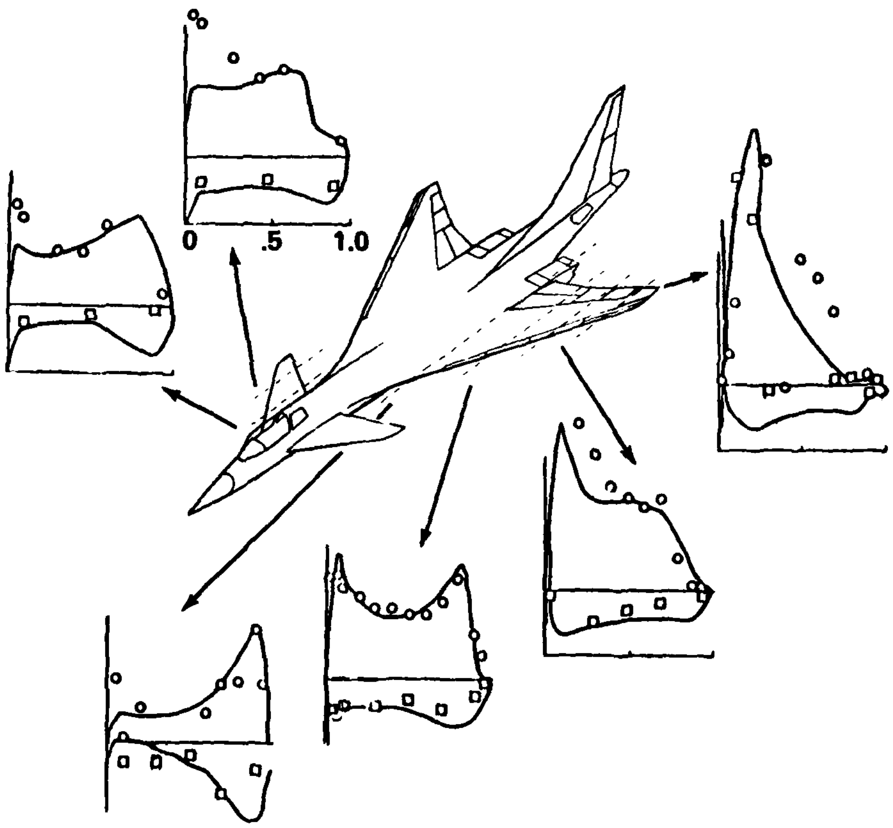

Figure 30. Wing-Body-Canard Pressures, Data-Analysis Comparison, Mach 0.9

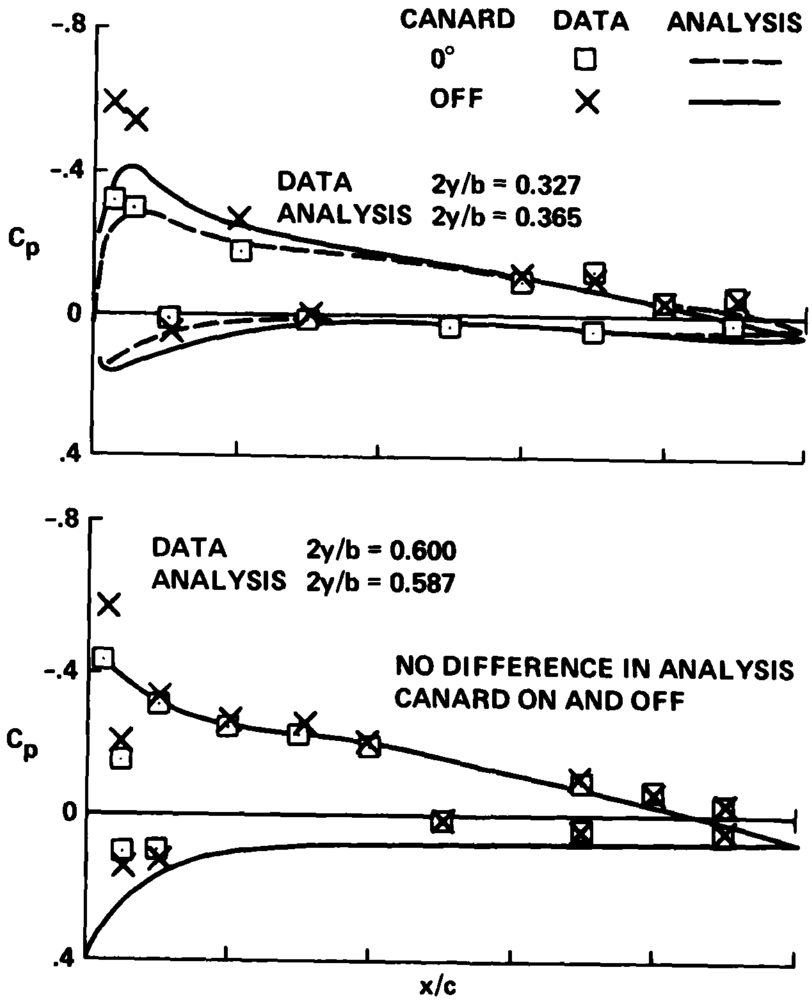

Figure 31. Wing Pressure Changes Due to Canard, Data-Analysis Comparisons, Mach 0.9.

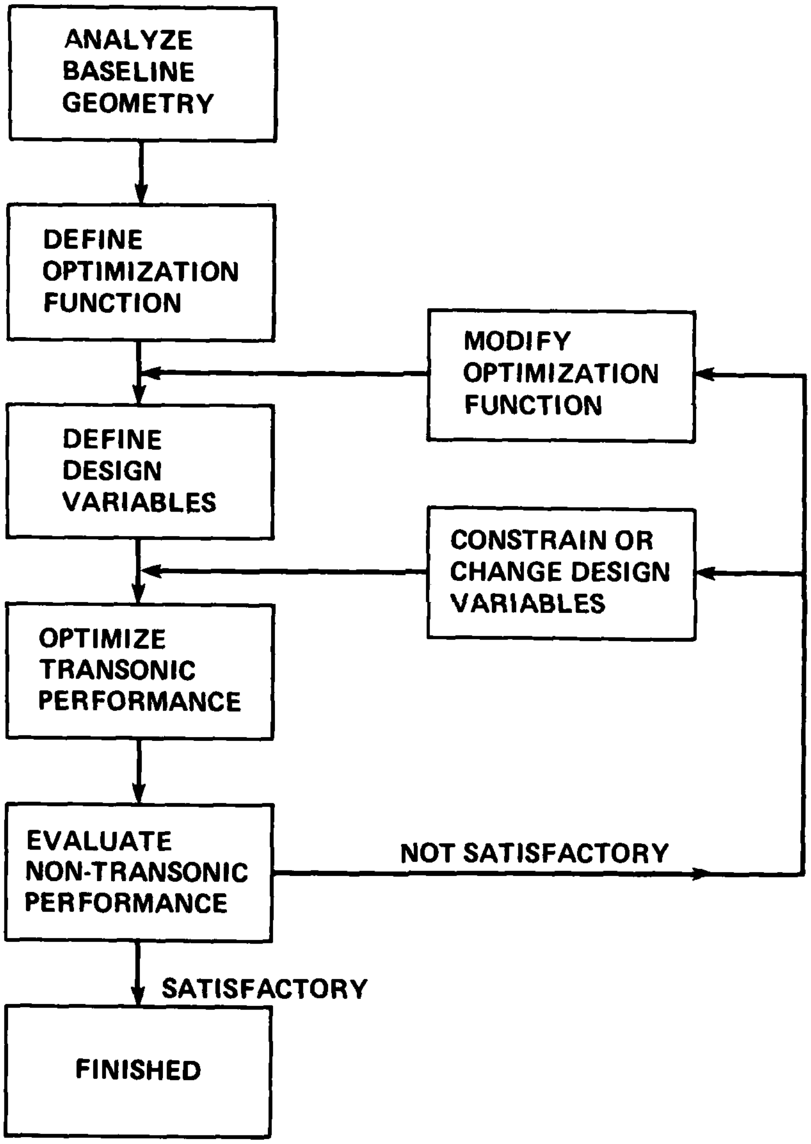

Figure 32. Design Procedure Outline.

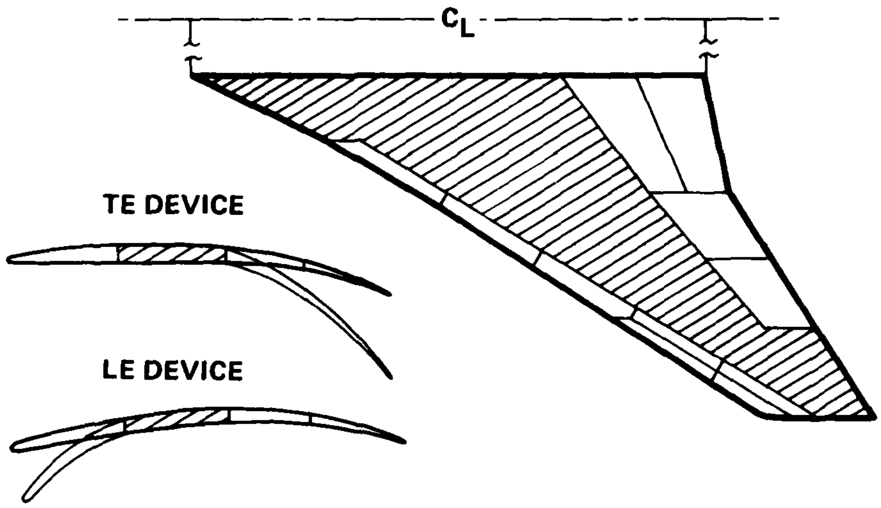

Figure 33. Variable Camber Segmentation for CDAF Wing Design.

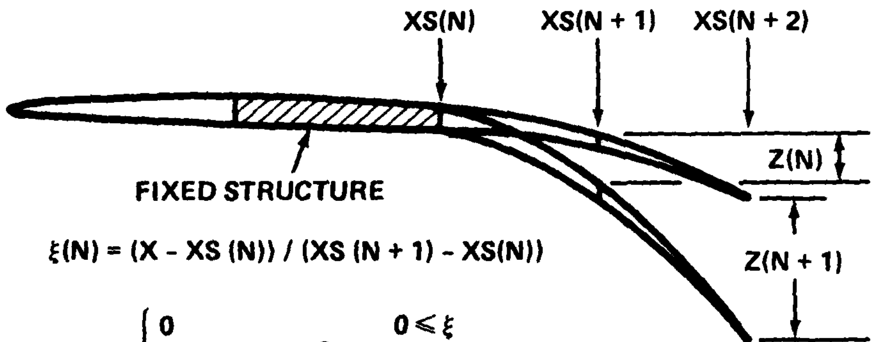

$$\xi(N) = (X - XS\,(N)) \,/\, (XS\,(N+1) - XS(N))$$

$$Z(N) = \begin{cases} 0 & 0 \leqslant \xi \\ A(1 - V(N))\,\xi^3(N) & 0 \leqslant \xi \leqslant 1 \\ B(1 - V(N))\,\xi\ (N) & 1 \leqslant \xi \end{cases}$$

WHERE

XS = CHORD STATION
Z = DEFLECTION
V = DESIGN VARIABLE
A,B = COEFFICIENTS FOR CONTOUR MATCHING

Figure 34. Variable Camber Model for Wing Design Optimization.

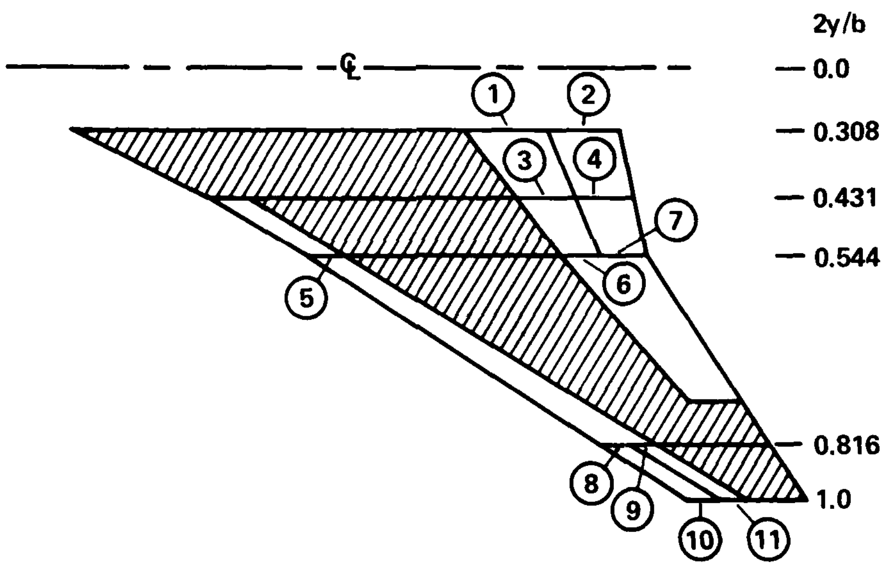

Figure 35. Camber Approach Design Variable Assignment.

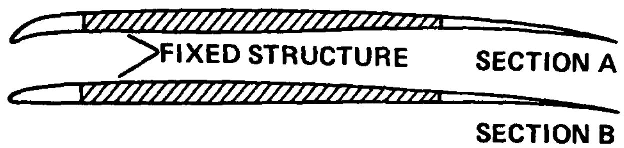

FOR WING SECTION N

$$Z(N) = ZA(N) \cdot (1 - V(N)) + ZB(N) \cdot V(N)$$

WHERE

- $Z(N)$ = WING SECTION ORDINATES AT SPAN STATION N
- $ZA(N)$ = WING SECTION A ORDINATES FOR SPAN STATION N
- $ZB(N)$ = WING SECTION B ORDINATES FOR SPAN STATION N
- $V(N)$ = DESIGN VARIABLE FOR SPAN STATION N

Figure 36. Wing Section Shape Model for Wing Design Optimization.

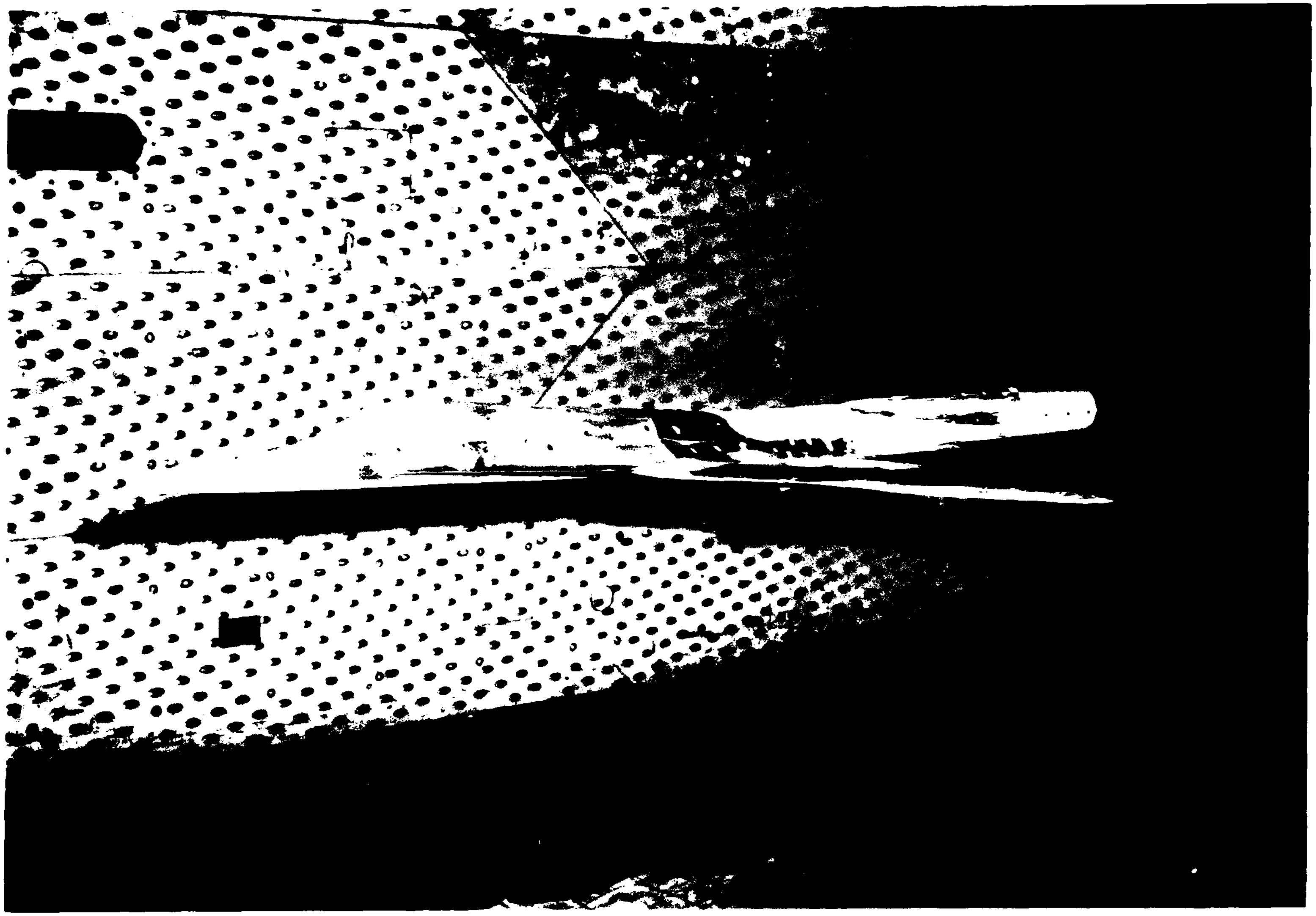

Figure 37. Wind Tunnel Model in AEDC PWT 16T Tunnel.

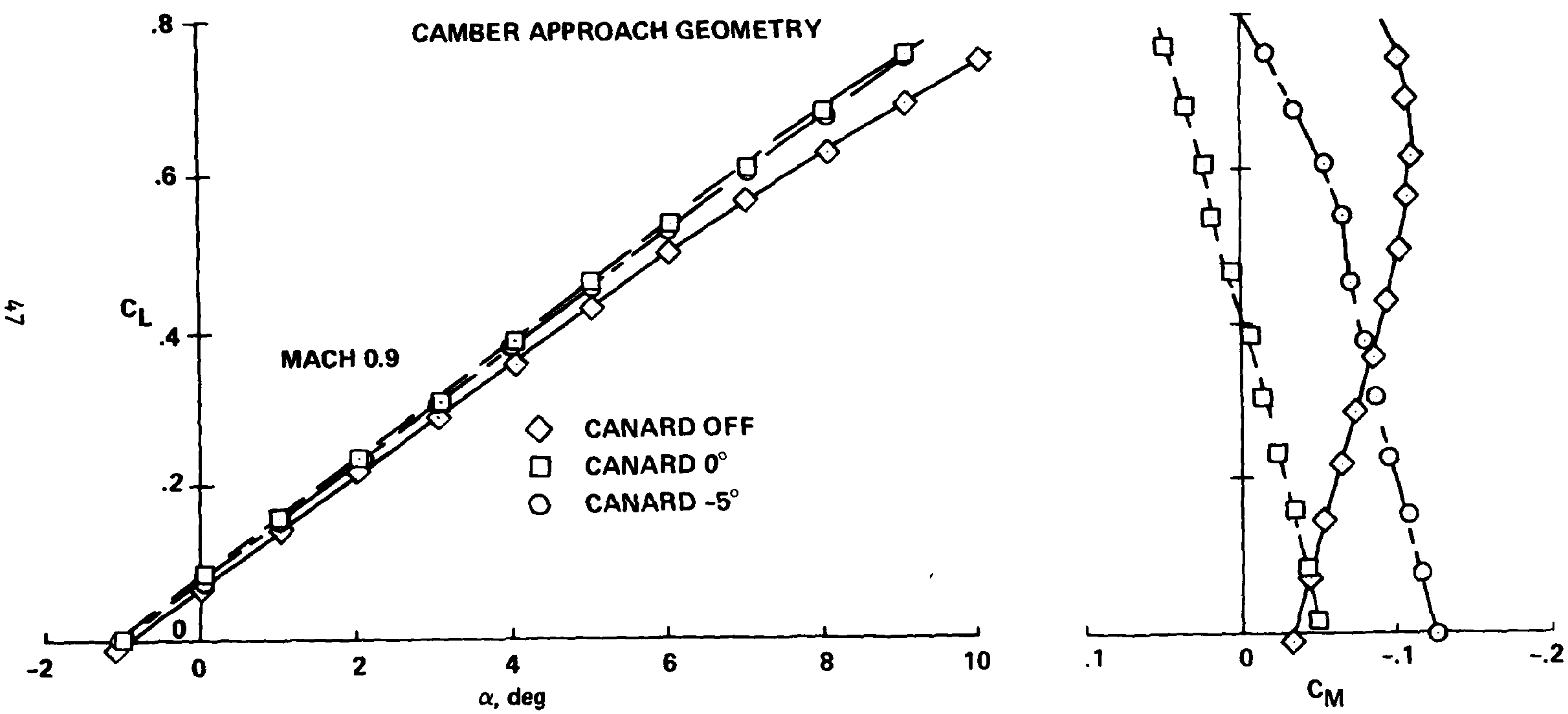

Figure 38. Test Results, Lift and Moment for Camber Approach Geometry, Mach 0.9.

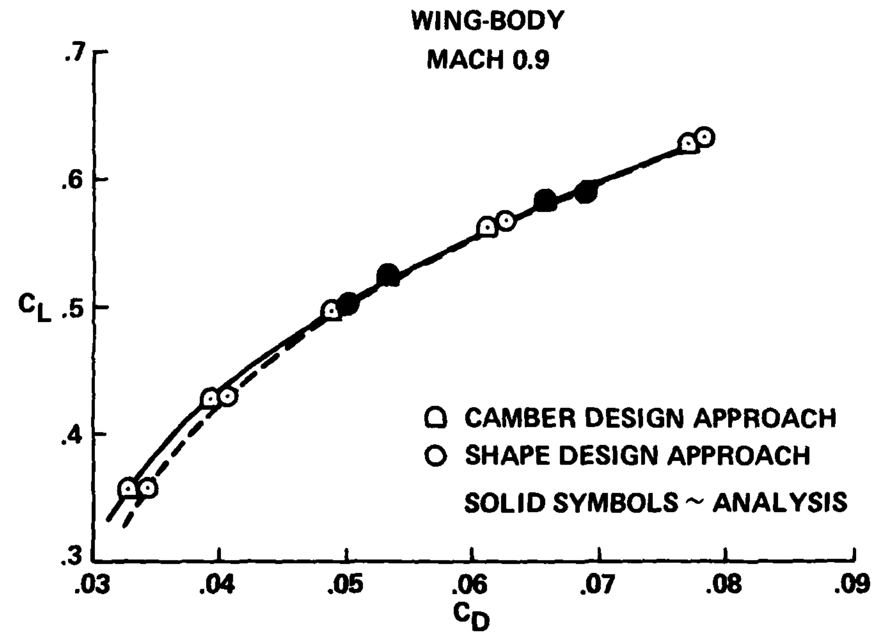

Figure 39. Wing-Body Drag, Data-Analysis Comparison, Mach 0.9.

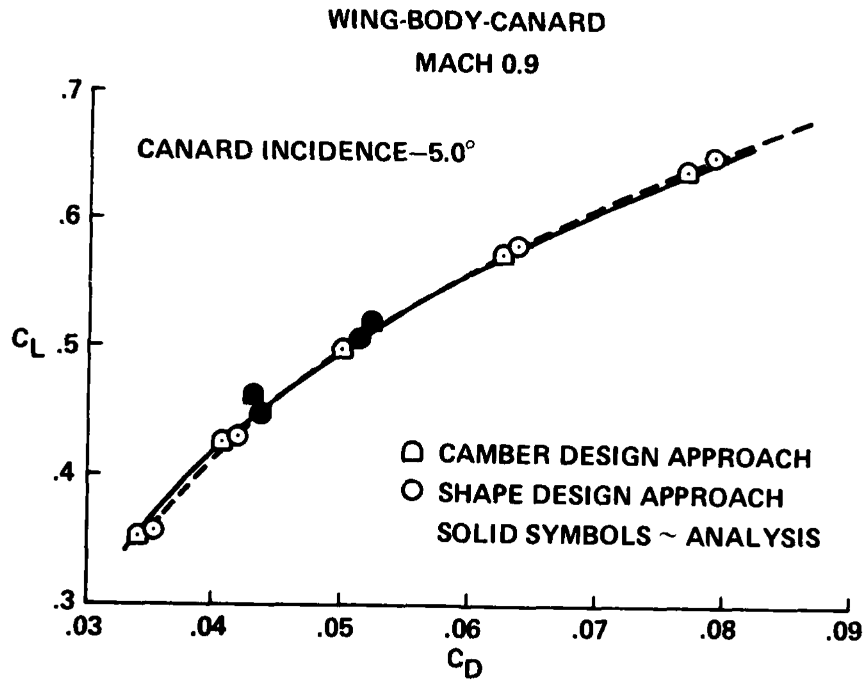

Figure 40. Wing-Body-Canard Drag, Data-Analysis Comparison, Mach 0.9.

*U.S.Government Printing Office: 1981 — 559-005/4022

DATE
FILMED

3 - 8